Weak lensing in the UNIONS survey

February 1, 2024

Joint ARGOS-TITAN-TOSCA meeting:
Cosmology and Statistics Days

Martin Kilbinger, France
CEA Paris-Saclay, CosmoStat

martin.kilbinger@cea.fr

Outline

- The UNIONS survey
- Weak gravitational lensing analysis
- First results

http://www.skysurvey.cc

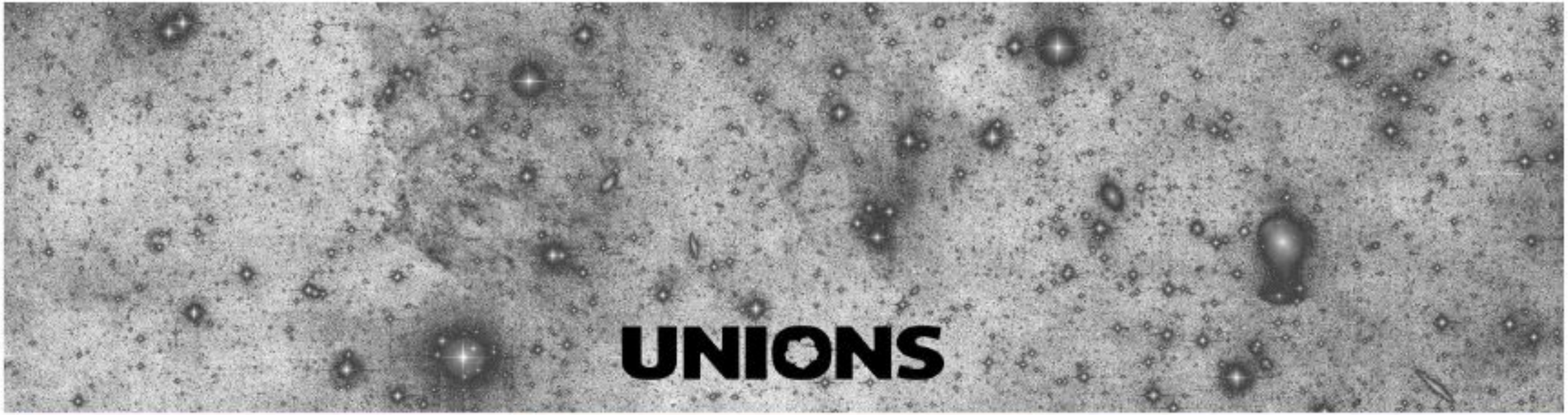

UNIONS: Ultra-violet Near-Infrared Optical Northern Survey
CFIS: Canada-France Imaging Survey

Large imaging survey (4,800 deg^2) in the Northern hemisphere with CFTH in optical bands *u*, *r* (CFIS), *i*, *z* (Pan-STARRS), *g*, *z* (HSC).
P.I.: Jean-Charles Cuillandre (DAp) & Alain McConnachie (Victoria/Canada)

- **Optical bands for Euclid for photometric redshifts**
- Weak lensing
- Milky Way dynamics
- Large-scale structure
- Galaxy evolution

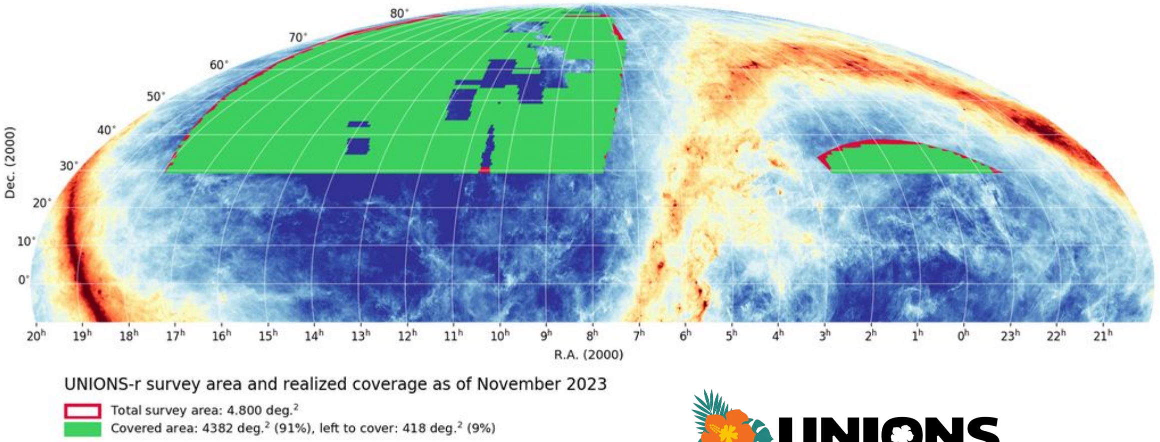

UNIONS

www.skysurvey.cc

UNIONS footprint & Euclid

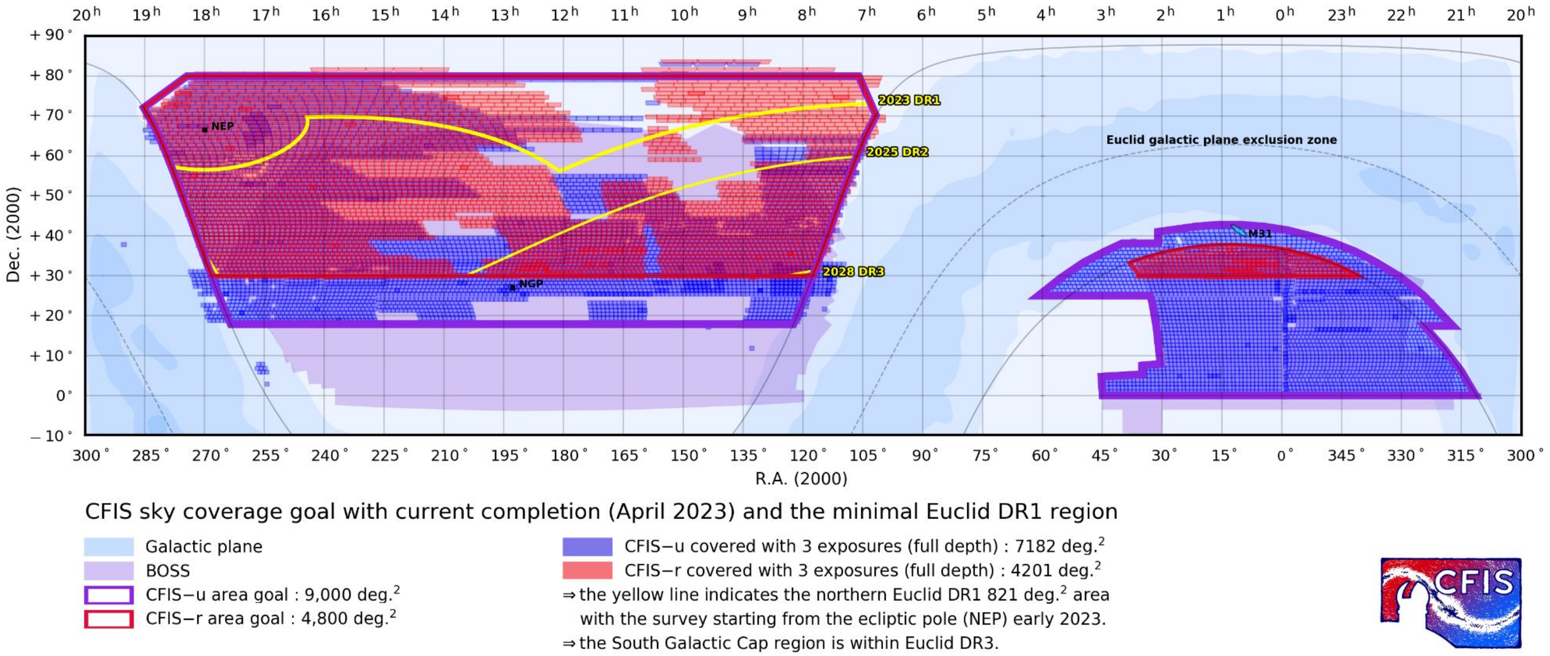

UNIONS footprint & Euclid

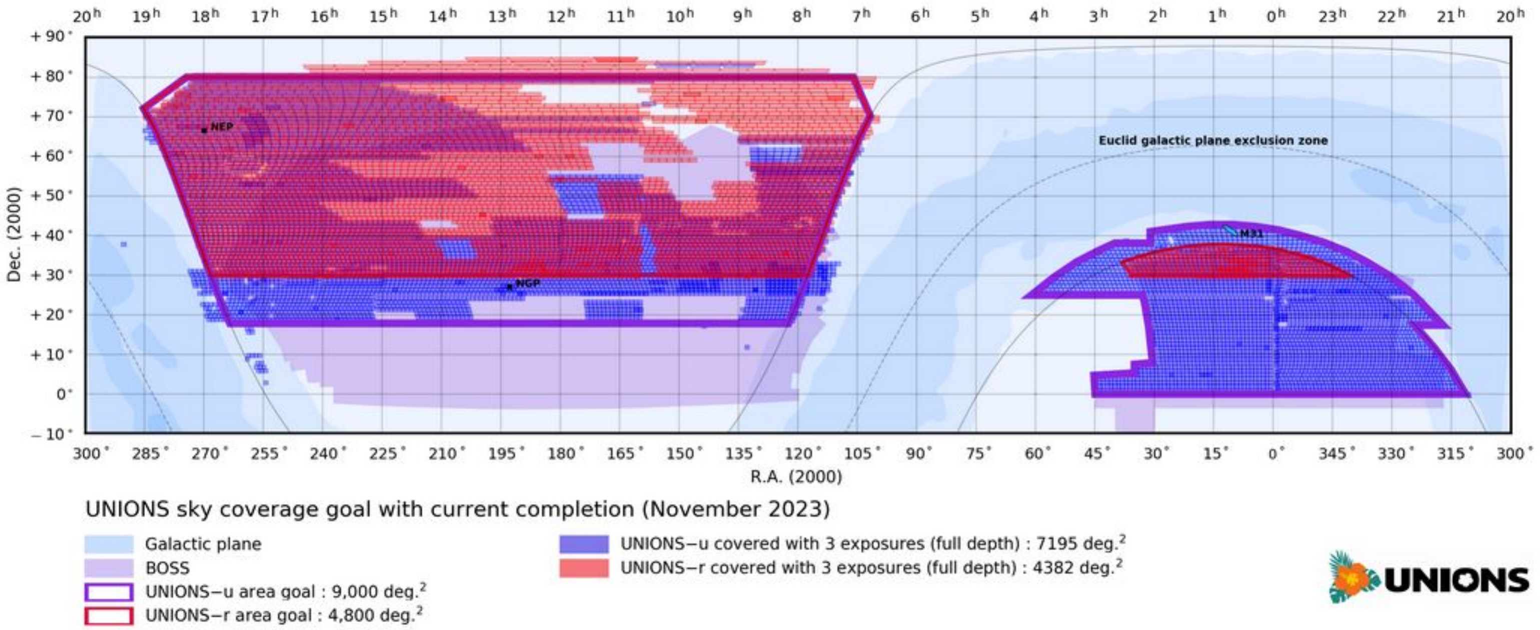

Sky coverage

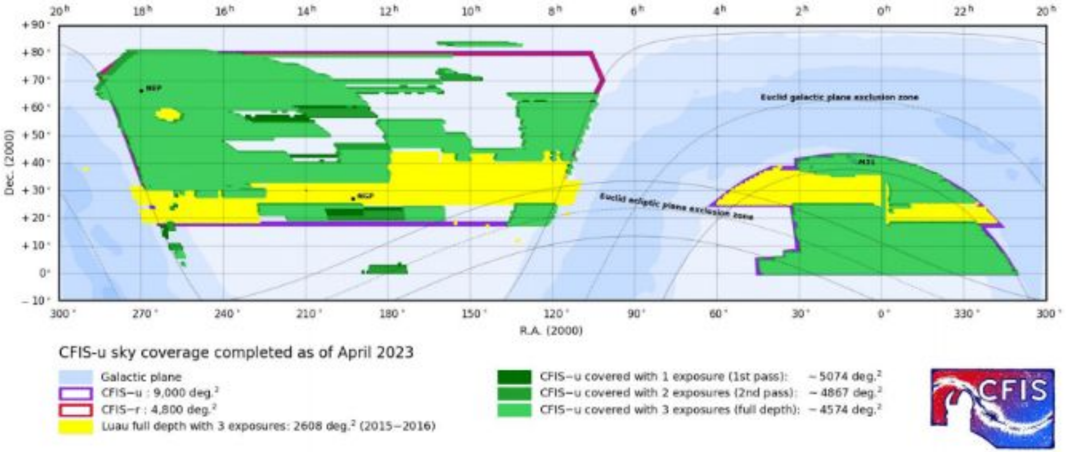

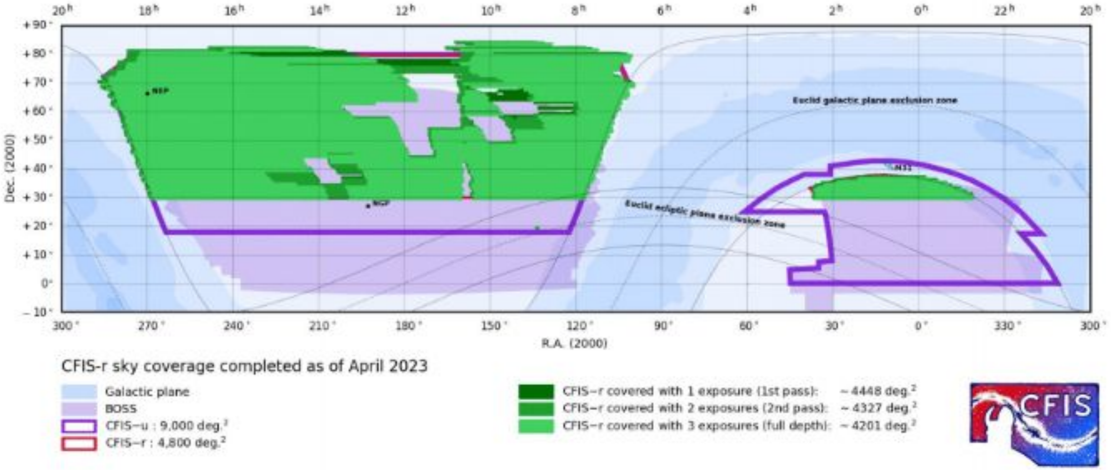

u = 80% complete
g = 75% complete
r = 87% complete
i = 100% complete (not full depth)
z = 64% complete (Subaru + Pan-STARRS)

Sky coverage

u = 80% complete
g = 75% complete
r = 87% complete
i = 100% complete (not full depth)
z = 64% complete (Subaru + Pan-STARRS)

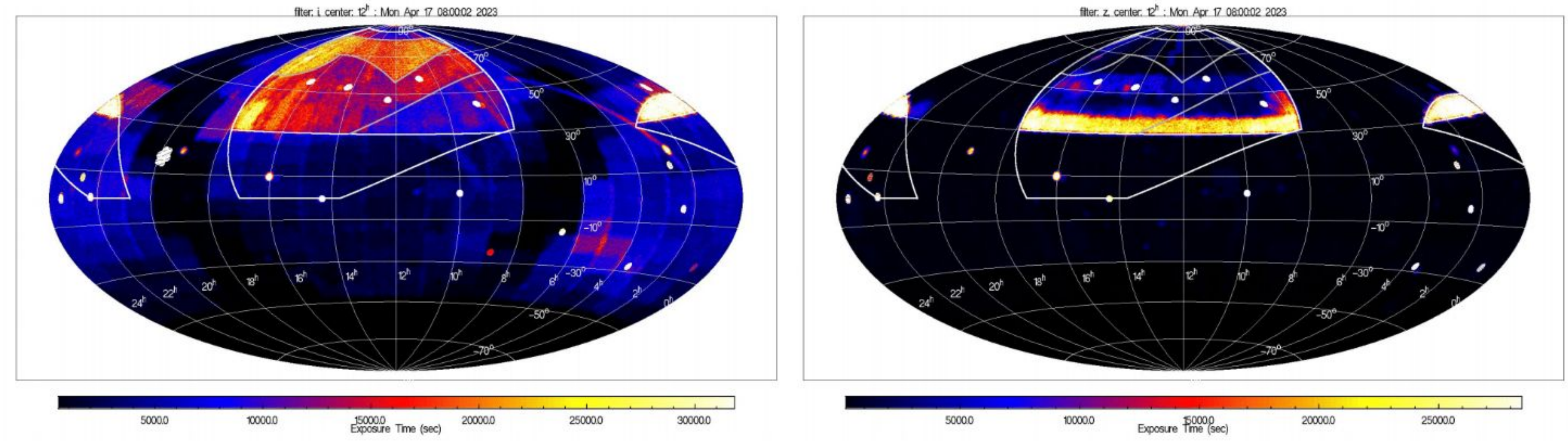

Pan-STARRS (2018-2025) : i-band (left) + z-band (right)

Sky coverage

u = 80% complete
g = 75% complete
r = 87% complete
i = 100% complete (not full depth)
z = 64% complete (Subaru + Pan-STARRS)

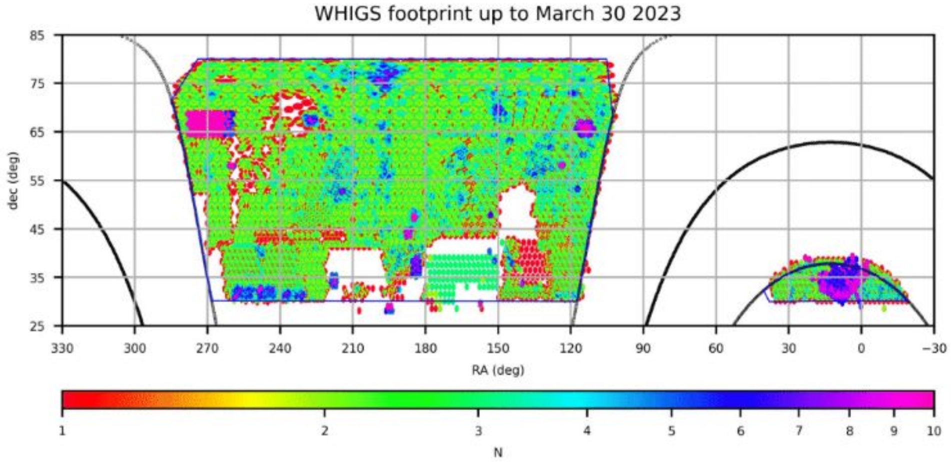

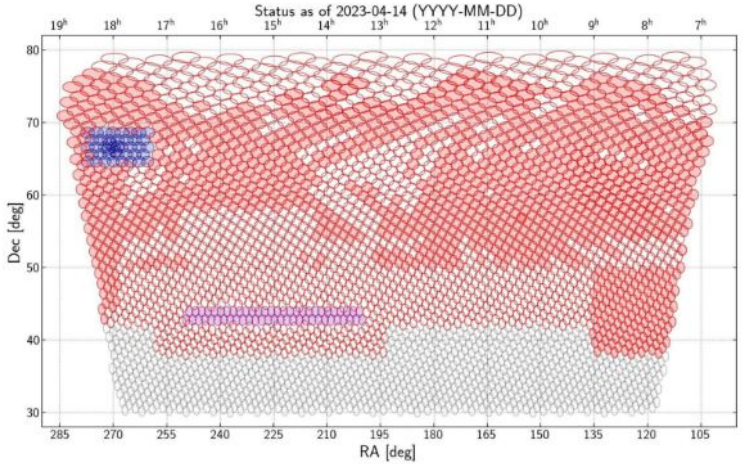

Subaru : g-band + z-band = WHIGS (2019-2024, left) + WISHES (2020-2024, right)

UNIONS/CFIS vs. SDSS

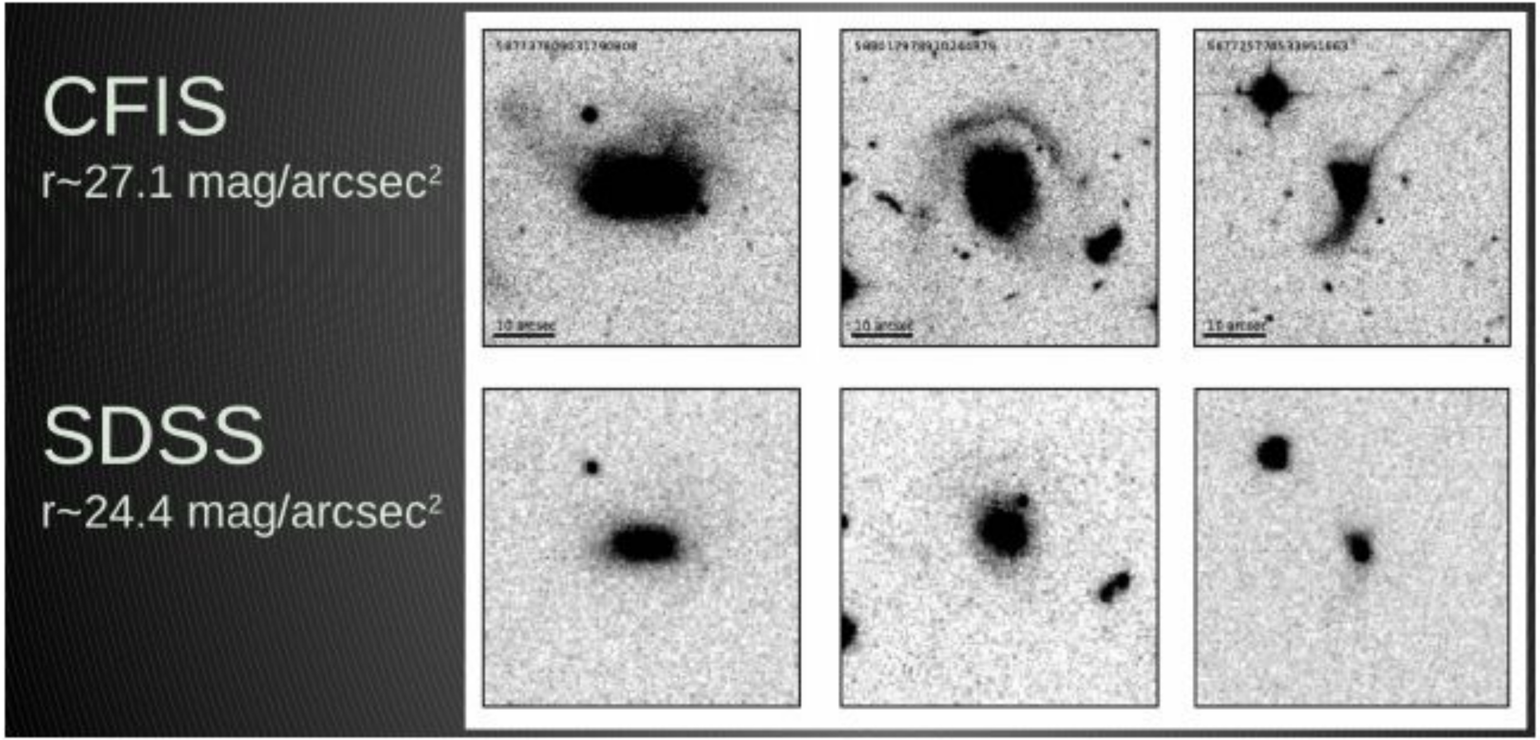

UNIONS/CFIS

Best wide-field imager on CFHT ever.

Improvements (2011 - 2014)

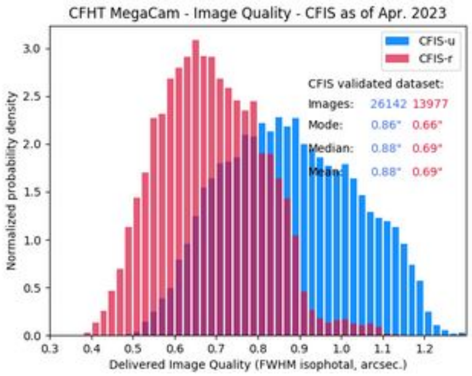

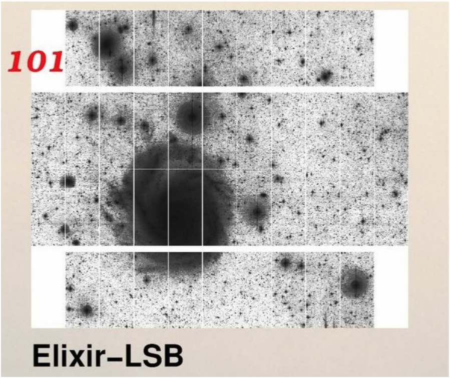

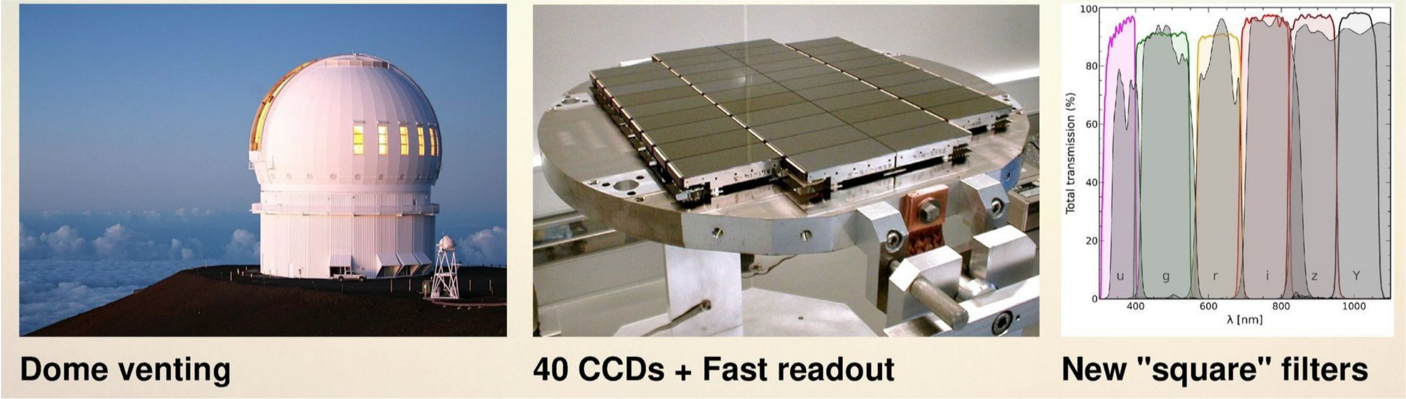

UNIONS is basically a static LSST in the North. Unique combination of depth, area, and image quality (unmatched before Euclid, Rubin, Roman, CSS-OS, WFST!)

UNIONS depth

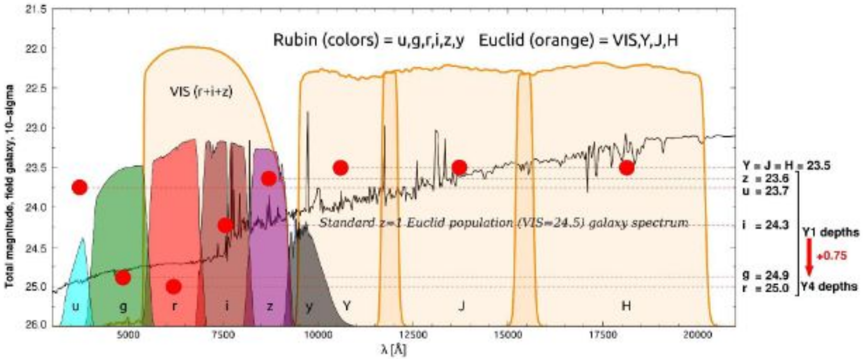

Photo-z depth metric proxy (for all): point source in 2 arcseconds diameter aperture, 10σ

- Euclid (median over the Euclid sky): *VIS=25.0, Y=J=H=23.5*
- DES in Euclid DR1/2/3: *g=24.7, r=24.4, i=23.8, z=23.1*
- UNIONS in Euclid DR1: *u=23.6, g=24.5, r=24.1, i=23.2, z=23.4*
- UNIONS in Euclid DR2: *u=23.6, g=24.5, r=24.1, i=23.4, z=23.4*
- UNIONS in Euclid DR3: *u=23.6, g=24.5, r=24.1, i=23.6, z=23.4*
- Rubin LSST* Y1 in Euclid DR2: *u=23.7, g=24.9, r=25.0, i=24.3, z=23.6*
- Rubin LSST* Y1 to Y4 in Euclid DR3: *u=24.4, g=25.6, r=25.7, i=25.0, z=24.3*

UNIONS ≈ LSST Year 1 depths

*Rubin-LSST main releases depth with point source PSF performance scaled to the 2” diam. metric

UNIONS and other surveys

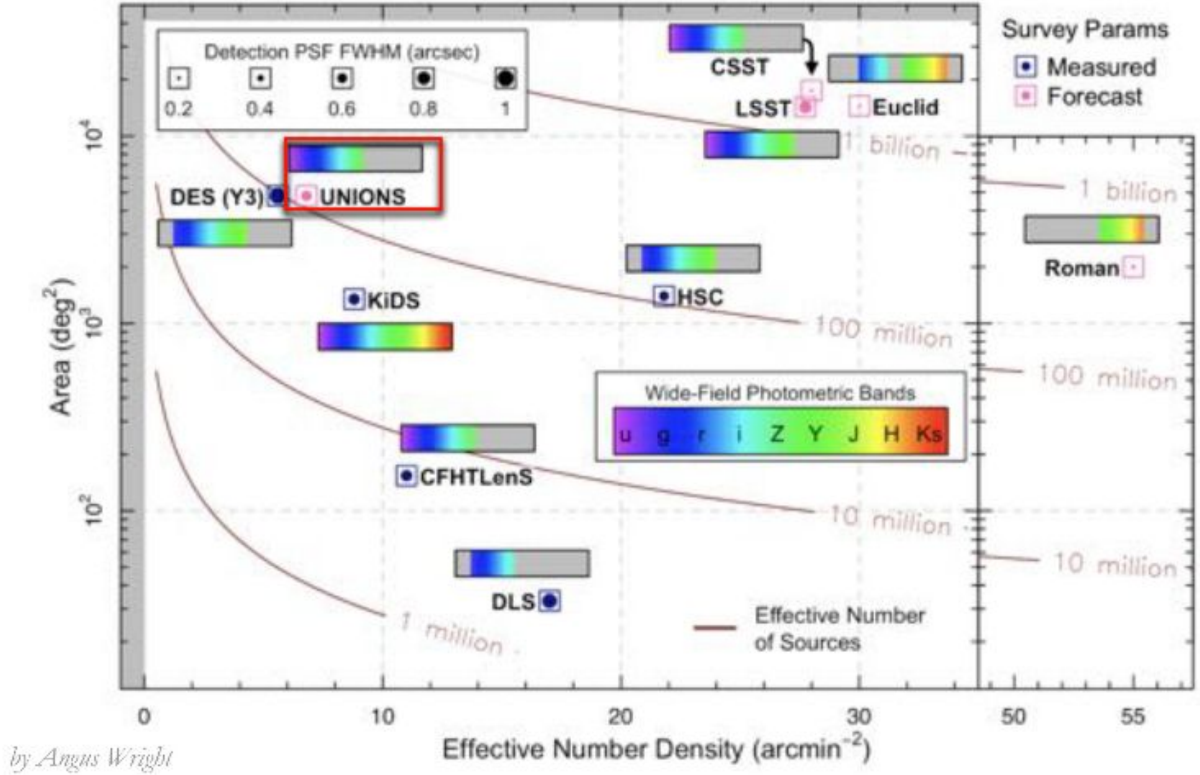

Weak gravitational lensing

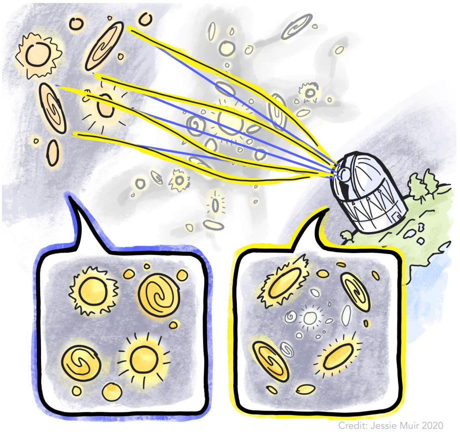

- Probe of (dark) matter distribution at large scales, and in clusters and galaxies
- Measures density amount and fluctuations amplitude ("σ_8 / S_8 tension")
- Dark-energy dominated epoch

Dvornik, Heymans, Asgari et al. 2022

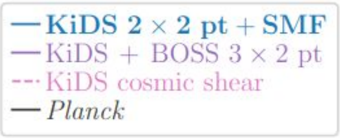

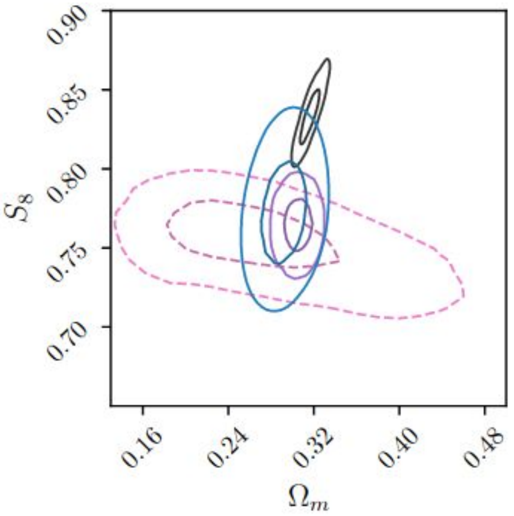

- "Weak" = galaxy shape distortions at %-level
  - ≪ intrinsic galaxy shapes
  - ≪ atmosphere & telescope distortions
- ➛ Need dedicated pipeline to process massive amounts of data for high-precision galaxy shape measurements + calibration

ShapePipe A modular weak-lensing processing and analysis pipeline

https://github.com/cosmostat/shapepipe

Farrens et al., 2022, A&A, 664, 141

ShapePipe

CI passing | pages-build-deployment passing | python 3.9 | release v1.0.1

ShapePipe is a galaxy shape measurement pipeline developed within the CosmoStat lab at CEA Paris-Saclay.

See the documentation for details on how to install and run ShapePipe.

Sacha Guerrini

Fabian Hervas Peters

ShapePipe

A modular weak-lensing processing and analysis pipeline

Software paper

Farrens et al., 2022, A&A, 664, 141

ShapePipe: A modular weak-lensing processing and analysis pipeline

S. Farrens[1] *, A. Guinot[2], M. Kilbinger[1], T. Liaudat[1], L. Baumont[1], X. Jimenez[3], A. Peel[4], A. Pujol[1], M. Schmitz[5], J.-L. Starck[1], and A. Z. Vitorelli[1]

[1] AIM, CEA, CNRS, Université Paris-Saclay, Université Paris Diderot, Sorbonne Paris Cité, F-91191 Gif-sur-Yvette, France
[2] Université de Paris, CNRS, Astroparticule et Cosmologie, F-75013 Paris, France
[3] Université Paris-Saclay, CNRS, ENS Paris-Saclay, Centre Borelli, 91190, Gif-sur-Yvette, France
[4] Institute of Physics, Laboratory of Astrophysics, Ecole Polytechnique Fédérale de Lausanne (EPFL), Observatoire de Sauverny, 1290 Versoix, Switzerland
[5] Université Côte d'Azur, Observatoire de la Côte d'Azur, CNRS, Laboratoire Lagrange, Bd de l'Observatoire, CS 34229, 06304 Nice Cedex 4, France

ABSTRACT

We present the first public release of ShapePipe, an open-source and modular weak-lensing measurement, analysis, and validation pipeline written in Python. We describe the design of the software and justify the choices made. We provide a brief description of all the modules currently available and summarise how the pipeline has been applied to real Ultraviolet Near-Infrared Optical Northern Survey data. Finally, we mention plans for future applications and development. The code and accompanying documentation are publicly available on GitHub.

Key words. Gravitational lensing: weak – Methods: data analysis

ShapePipe

Goals

- Modular
- Easy
- Fast (enough)
- Robust

Code installation

- Conda
- Docker (in prep)
- CD/CI

Three components

Pipeline

- Arguments & config
- I/O
- Job handling (MPI, SMP)
- Errors & logging

Modules

- WL data processing
- Book-keeping

Utilities

- Scripts
- Tools
- Survey-specific content

Image processing with ShapePipe

Input images are pre-processed (calibrated for astrometry and photometry)

Main processing

- Mask
- Detect objects
  - Star candidates on single exposures
  - Galaxy candidates and stacks
- Select stars
- Create PSF model
- Interpol PSF model to galaxy positions
- Validate PSF model
- Measure galaxy shapes including calibration information

Post-processing

- Galaxy selection
- Apply calibration
- Systematic checks (e.g null tests)

Image processing with ShapePipe

Input images are pre-processed (calibrated for astrometry and photometry)

Main processing

- **Mask**
- Detect objects
  - **Star candidates** on single exposures
  - Galaxy candidates and stacks
- Select stars
- Create PSF model
- Interpol PSF model to galaxy positions
- Validate PSF model
- Measure galaxy shapes including calibration information

Post-processing

- Galaxy selection
- Apply calibration
- Systematic checks (e.g null tests)

Masking

Image artefacts: spurious detections as galaxies, contaminations to weak-lensing shear (correlations).

We mask:

- Halos and diffraction spikes of bright halos (from Guide Star Catalogue GSC II)
- Messier & NGC objects
- CCD borders

Already masked in pre-processing:

- cosmic rays (somewhat)
- bad columns

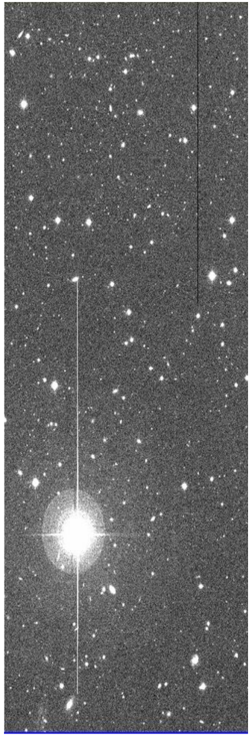

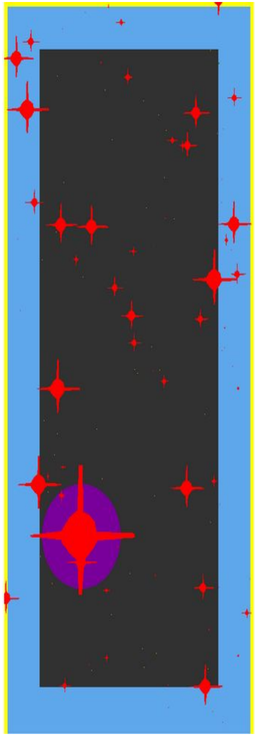

Masking: example

Detections in a 50 deg^2 area — Stacked image — NGC 2366 (UGC 3851) — Add mask

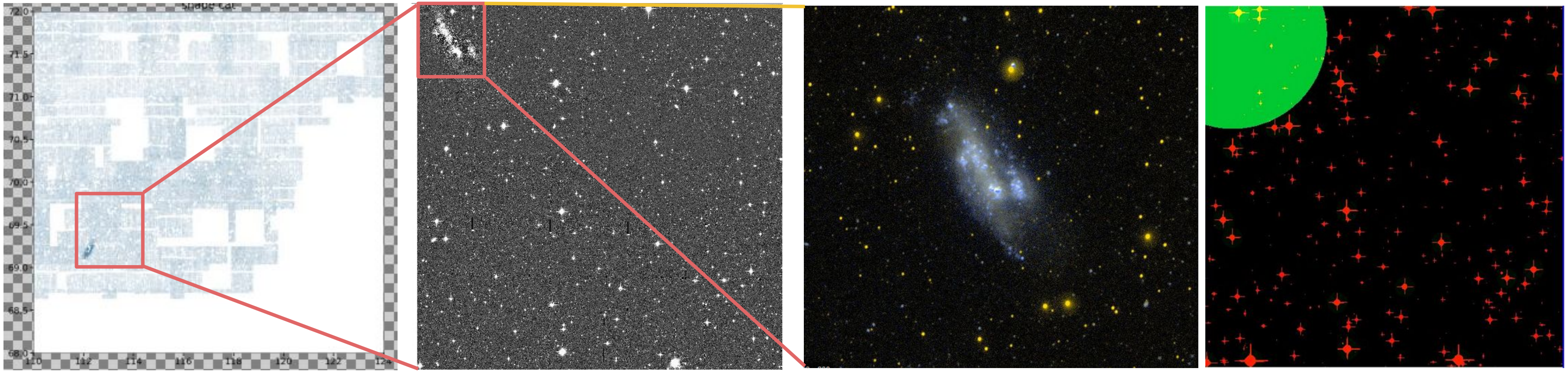

Knots in nearby galaxies create spurious detections as WL galaxies, need to be removed from analysis.

Star selection

Use stars to create PSF model.

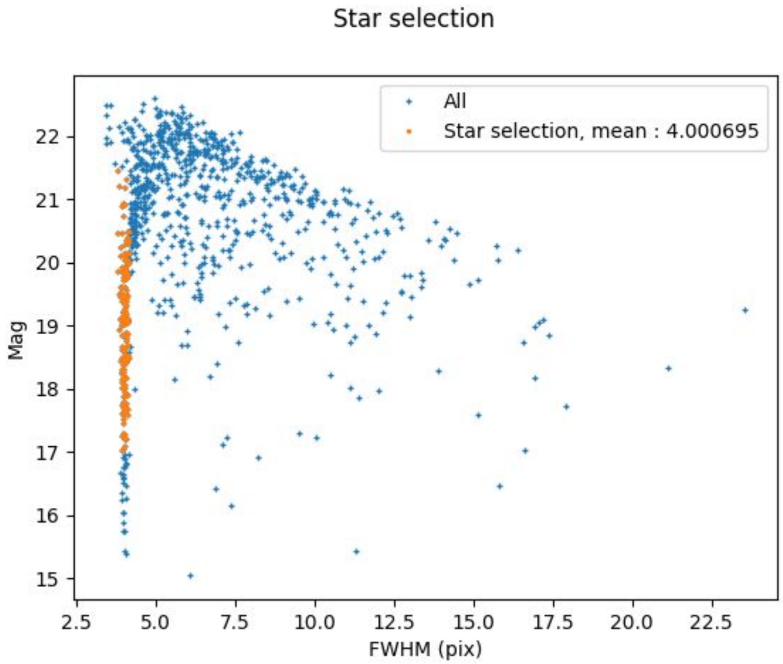

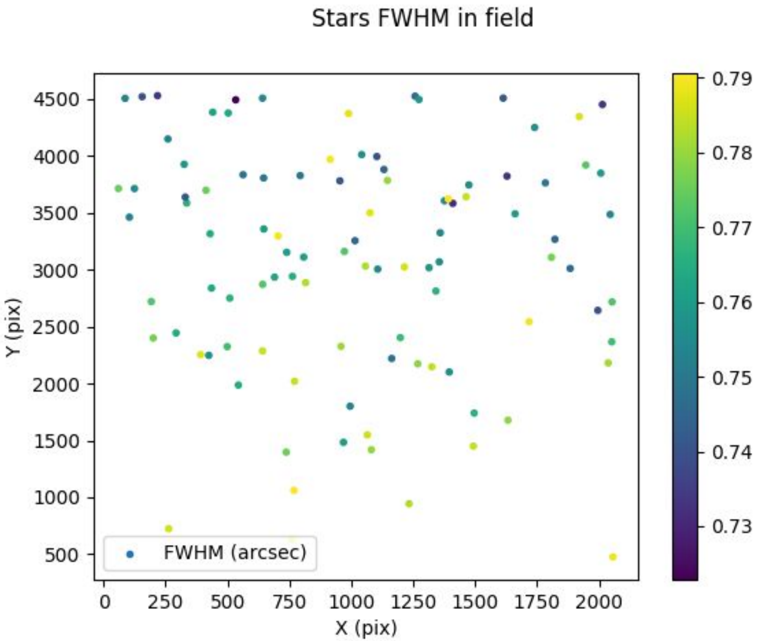

PSF model

Two models can be used:

- PSFEx, Bertin et al. 2011
- MCCD, Liaudat et al. 2021, [A&A, 646, A27]

Stacked MegaCAM focal plane

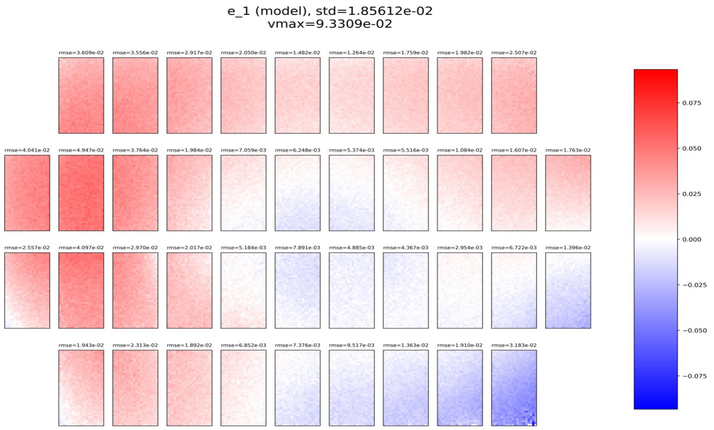

PSF ellipticity component 1

PSF ellipticity residual component 1

PSF diagnostics

The standard equation for PSF leakage for a galaxy is

$$e_i^{\text{obs}} = (1+m)\gamma_i + c_i + \alpha e_i^{\text{psf}}.$$

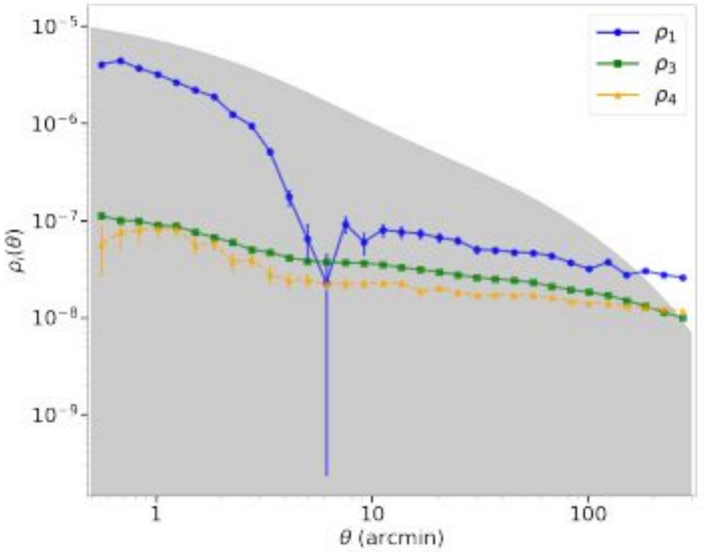

From this we derive the rho statistics as additive terms to the shear two-point correlation function. Their contribution propagates to cosmological parameters.

$$\rho_1(\theta) = \langle \delta e^*_{\text{PSF}}(\boldsymbol{\theta}')\delta e_{\text{PSF}}(\boldsymbol{\theta}'+\boldsymbol{\theta})\rangle;$$

$$\rho_2(\theta) = \langle e^*_{\text{PSF}}(\boldsymbol{\theta}')\delta e_{\text{PSF}}(\boldsymbol{\theta}'+\boldsymbol{\theta})\rangle;$$

$$\rho_3(\theta) = \left\langle \left(e^*_{\text{PSF}}\frac{\delta T_{\text{PSF}}}{T_{\text{PSF}}}\right)(\boldsymbol{\theta}') \left(e_{\text{PSF}}\frac{\delta T_{\text{PSF}}}{T_{\text{PSF}}}\right)(\boldsymbol{\theta}'+\boldsymbol{\theta})\right\rangle;$$

$$\rho_4(\theta) = \left\langle \delta e^*_{\text{PSF}}(\boldsymbol{\theta}') \left(e_{\text{PSF}}\frac{\delta T_{\text{PSF}}}{T_{\text{PSF}}}\right)(\boldsymbol{\theta}'+\boldsymbol{\theta})\right\rangle;$$

$$\rho_5(\theta) = \left\langle e^*_{\text{PSF}}(\boldsymbol{\theta}') \left(e_{\text{PSF}}\frac{\delta T_{\text{PSF}}}{T_{\text{PSF}}}\right)(\boldsymbol{\theta}'+\boldsymbol{\theta})\right\rangle.$$

PSF leakage

The standard equation for PSF leakage for a galaxy is

$$e_i^{\mathrm{obs}} = (1+m)\gamma_i + c_i + \alpha e_i^{\mathrm{psf}}. \tag{1}$$

Neglecting the shear (which is fine since later we will look at large samples), so far we have written the PSF leakage part as a matrix equation,

$$e_i^{\mathrm{obs}} = \sum_j \alpha_{ij} e_j^{\mathrm{psf}} + c_i \quad \text{or} \quad \boldsymbol{e}^{\mathrm{obs}} = \boldsymbol{\alpha}\boldsymbol{e}^{\mathrm{psf}} + \boldsymbol{c}, \tag{2}$$

and fitted the four components of $\boldsymbol{\alpha}$ independently.

PSF leakage into galaxy ellipticity

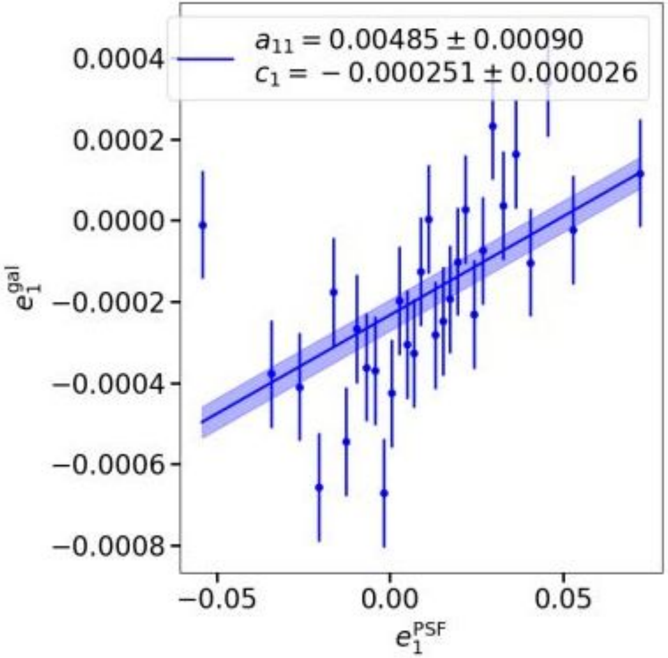

(see also Zhang et al. (2022), HSC-Y3 papers (2023))

PSF leakage

Kitching & Deshpande (2022), consistent relations between spin-2 quantities.
To second order:

$$e_1^{\rm obs} = q_{111}\left[e_1^{\rm psf}\right]^2 + q_{122}\left[e_2^{\rm psf}\right]^2 + q_{112}e_1^{\rm psf}e_2^{\rm psf} + m_{11}e_1^{\rm psf} + m_{12}e_2^{\rm psf} + c_1;$$
$$e_2^{\rm obs} = q_{222}\left[e_2^{\rm psf}\right]^2 + q_{211}\left[e_1^{\rm psf}\right]^2 + q_{212}e_1^{\rm psf}e_2^{\rm psf} + m_{22}e_2^{\rm psf} + m_{12}e_1^{\rm psf} + c_2. \quad (3)$$

- Coupled equations, need to do joint fits as function of both PSF ellipticity components
- Six quadratic terms
- One mixed linear term $m_{12} = m_{21}$

PSF leakage

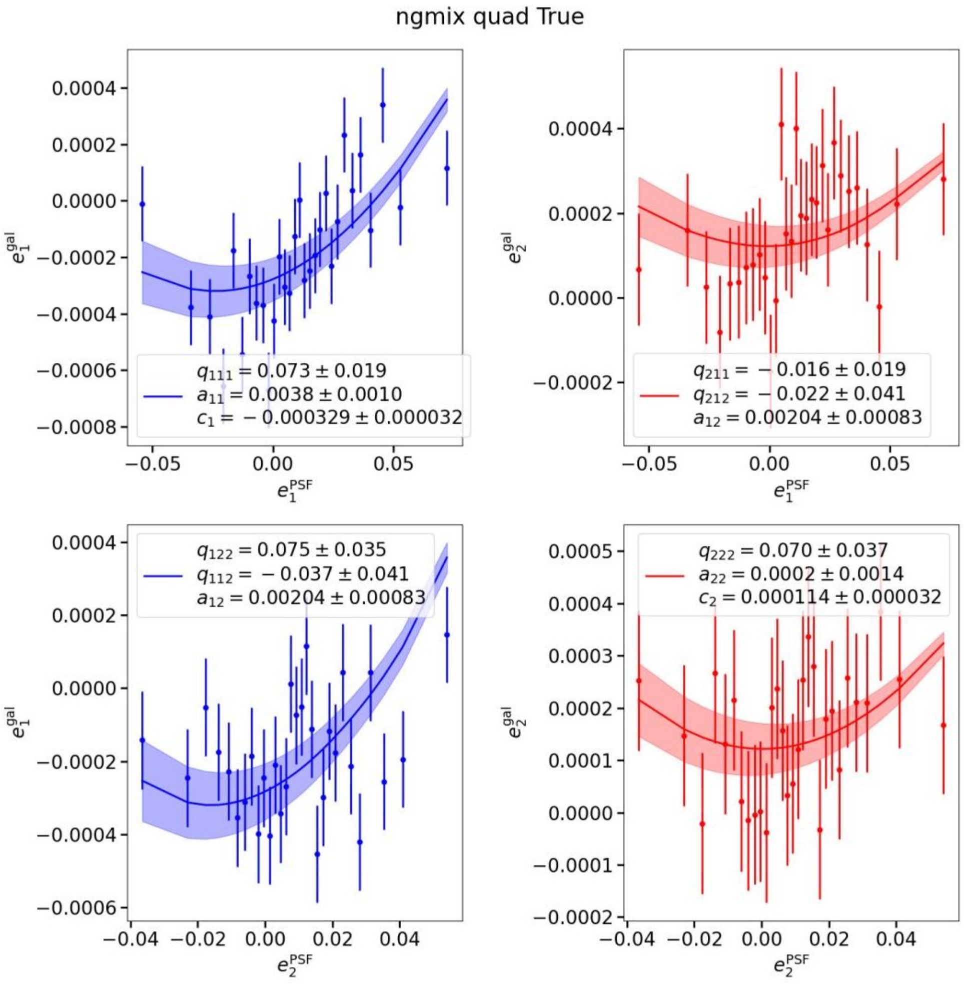

ngmix quad True
$q_{111} = 0.073 \pm 0.019$
$a_{11} = 0.0038 \pm 0.0010$
$c_1 = -0.000329 \pm 0.000032$
$q_{211} = -0.016 \pm 0.019$
$q_{212} = -0.022 \pm 0.041$
$a_{12} = 0.00204 \pm 0.00083$
$q_{122} = 0.075 \pm 0.035$
$q_{112} = -0.037 \pm 0.041$
$a_{12} = 0.00204 \pm 0.00083$
$q_{222} = 0.070 \pm 0.037$
$a_{22} = 0.0002 \pm 0.0014$
$c_2 = 0.000114 \pm 0.000032$
$e_1^{\rm gal}$
$e_2^{\rm gal}$
$e_1^{\rm PSF}$
$e_2^{\rm PSF}$

PSF diagnostics

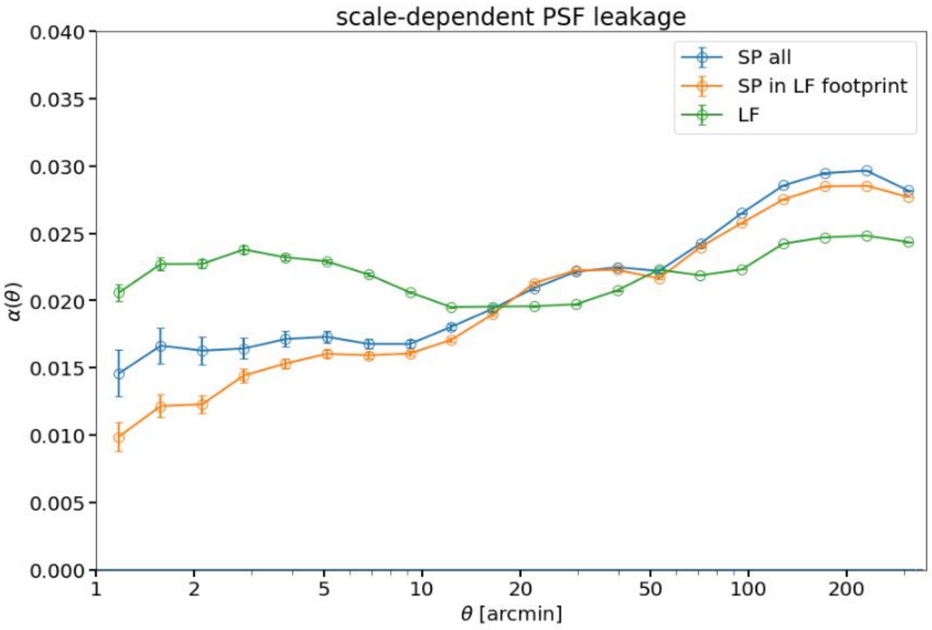

Observed ellipticity

$$e_i^{\rm obs} = (1+m)\gamma_i + c_i + \alpha e_i^{\rm psf}.$$

Leakage function

$$\alpha(\theta) = \frac{\xi_+^{\rm gp}(\theta) - \langle e_{\rm gal}\rangle^* \langle e_{\rm PSF}\rangle}{\xi_+^{\rm pp}(\theta) - |\langle e_{\rm PSF}\rangle|^2}.$$

Galaxy shape measurement

- Simple model for galaxy light profile (Gaussian)
- Convolve model with PSF
- Fit to observed galaxy, minimise to measure shape parameters
- ngmix (DES; E. Sheldon et al.), weighted moments

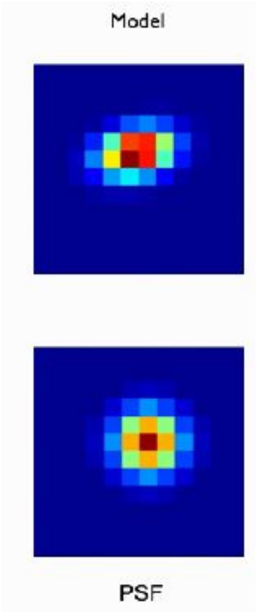

Convolve

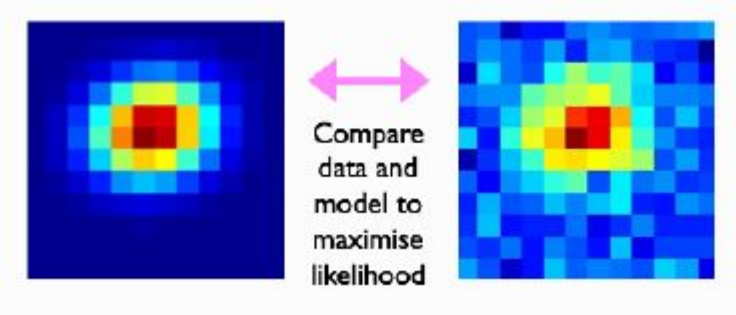

(Meta-)Calibration

- Weak-lensing shapes are biased (noise, wrong model or PSF, blended galaxies.
- Multiplicative bias **R** most important:

$$\boldsymbol{\gamma}^{\rm obs} = \mathbf{R}\, \boldsymbol{\gamma}^{\rm true} + \boldsymbol{c}$$

- Interpret **R** as response of the observed shape to a (small) shear:

$$\mathbf{R} = d\boldsymbol{\gamma}^{\rm obs} / d\boldsymbol{\gamma}^{\rm true} \approx [\, \boldsymbol{\gamma}^{\rm obs}(\boldsymbol{\gamma}^{\rm true} + \delta\boldsymbol{\gamma}) - \boldsymbol{\gamma}^{\rm obs}(\boldsymbol{\gamma}^{\rm true} - \delta\boldsymbol{\gamma}) \,] / [\, 2\, \delta\boldsymbol{\gamma} \,]$$

- **R** can be measured by applying small artificial shear $\boldsymbol{\delta\gamma}$ to each observed galaxy.

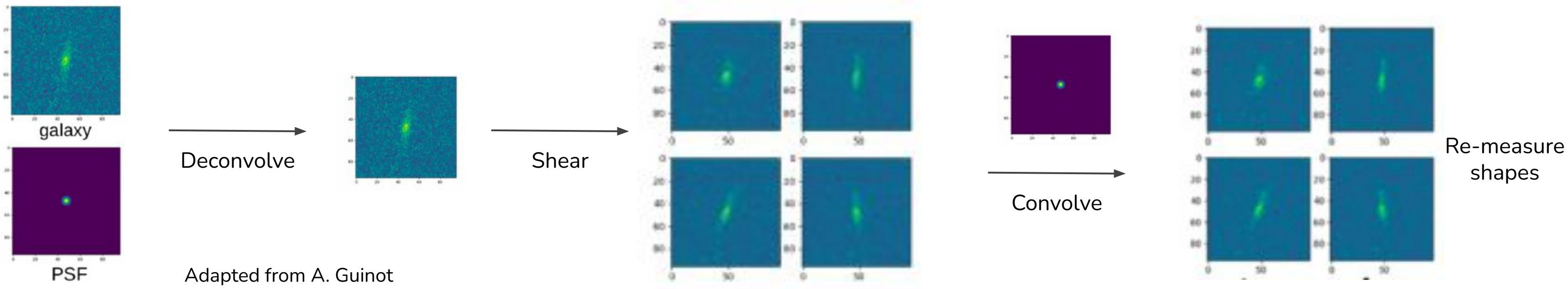

Adapted from A. Guinot

Metacalibration response matrix

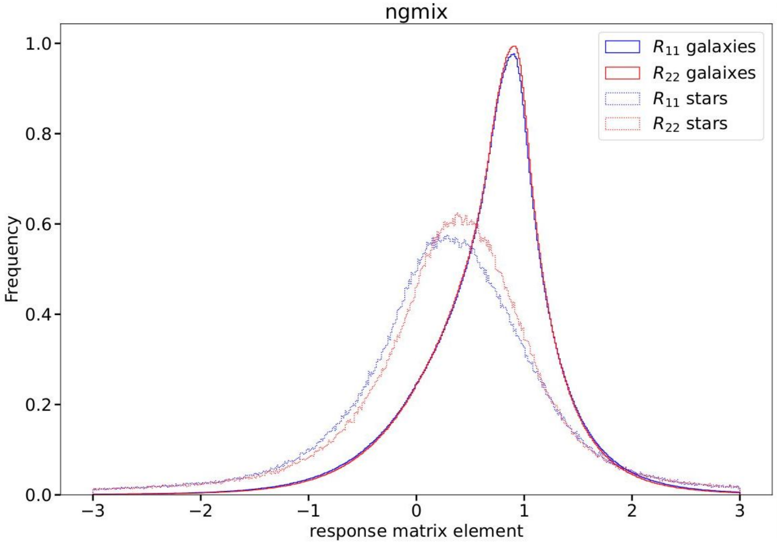

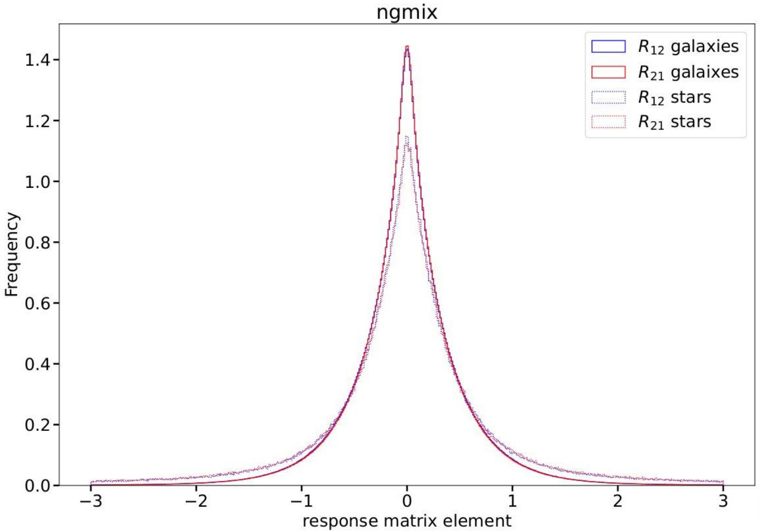

Galaxies: <R>~0.7, 30% bias. Stars: <R>~0-0.2, stars are point sources, no/small response to shear.

Some first results

- Mass maps, cluster convergence & masses
- Peak counts
- Intrinsic galaxy alignment
- Dark matter halo shapes

Future publications

- Blinded (redshift distribution)
- Two pipelines (ShapePipe and *lens*fit)

Mass maps

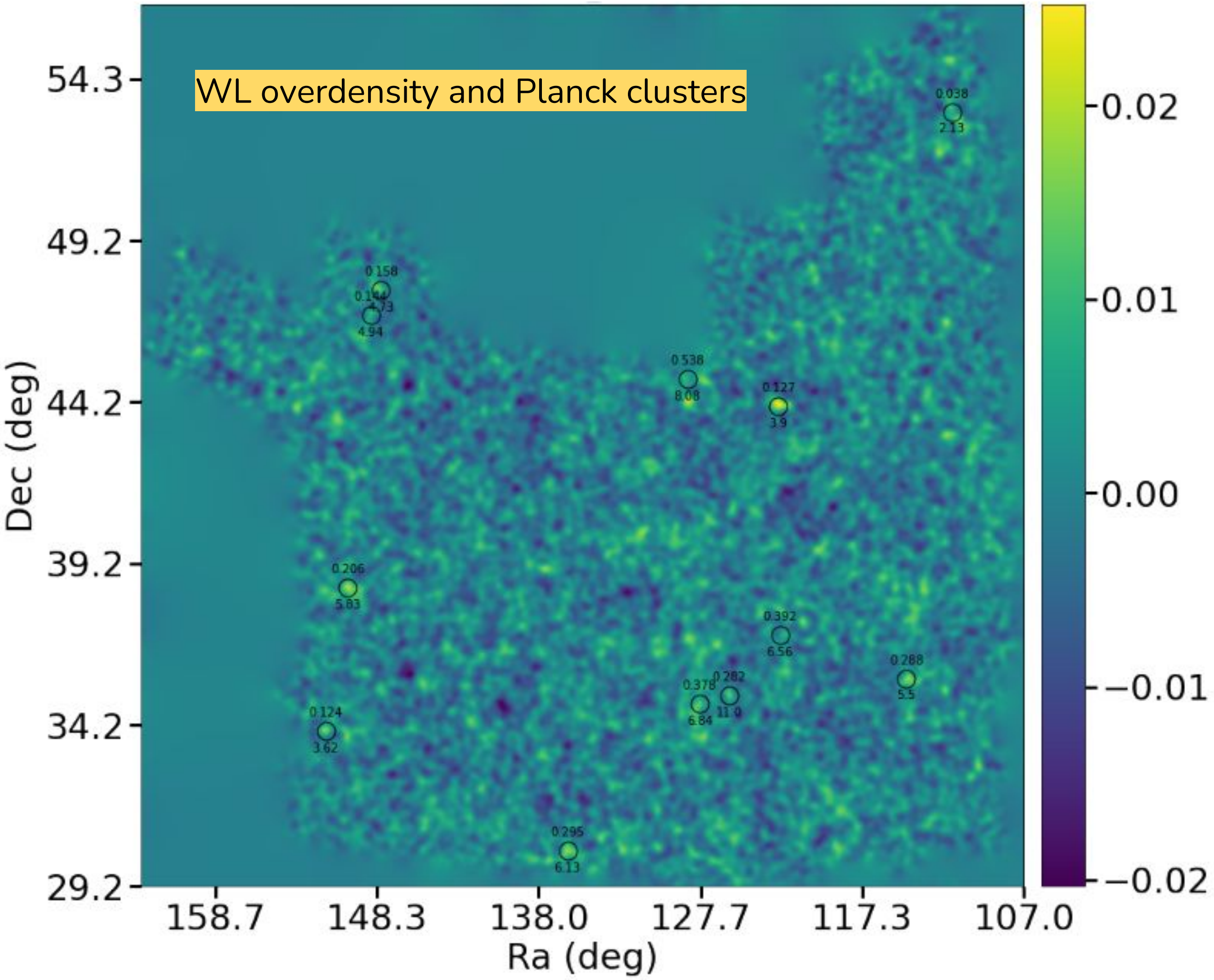

Guinot et al. (2022)

Mass

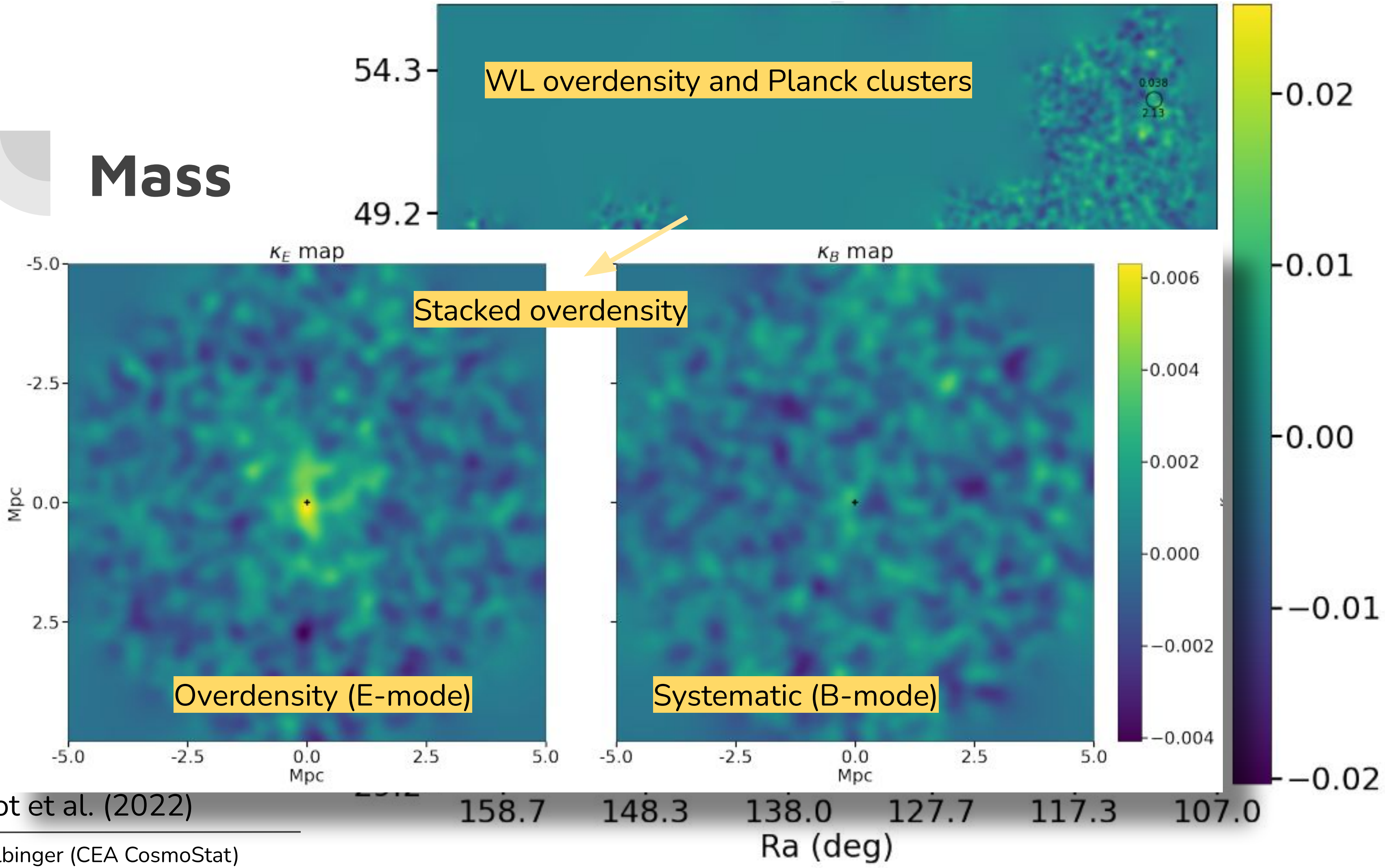

Guinot et al. (2022)

Mass

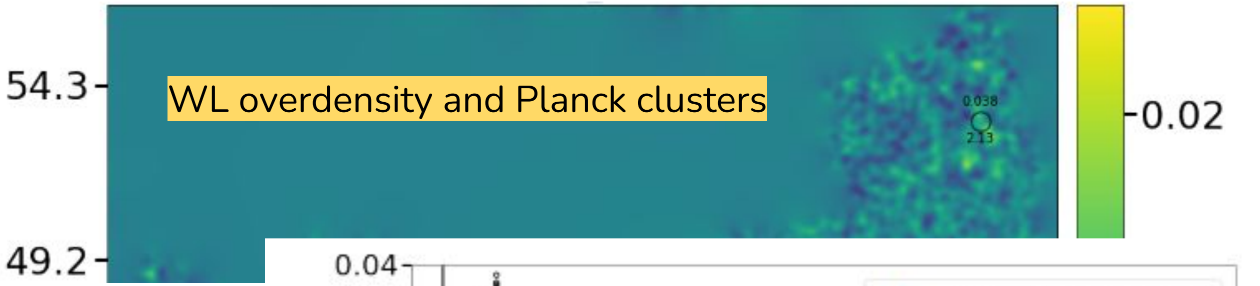

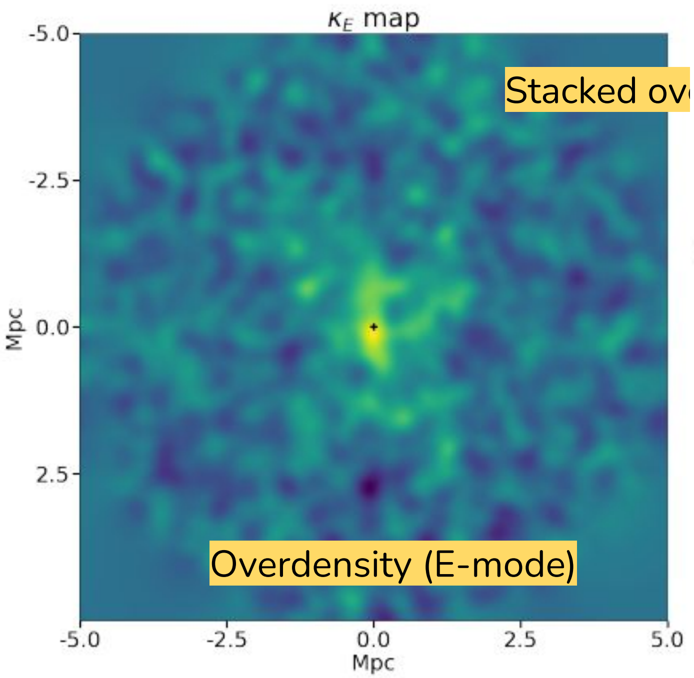

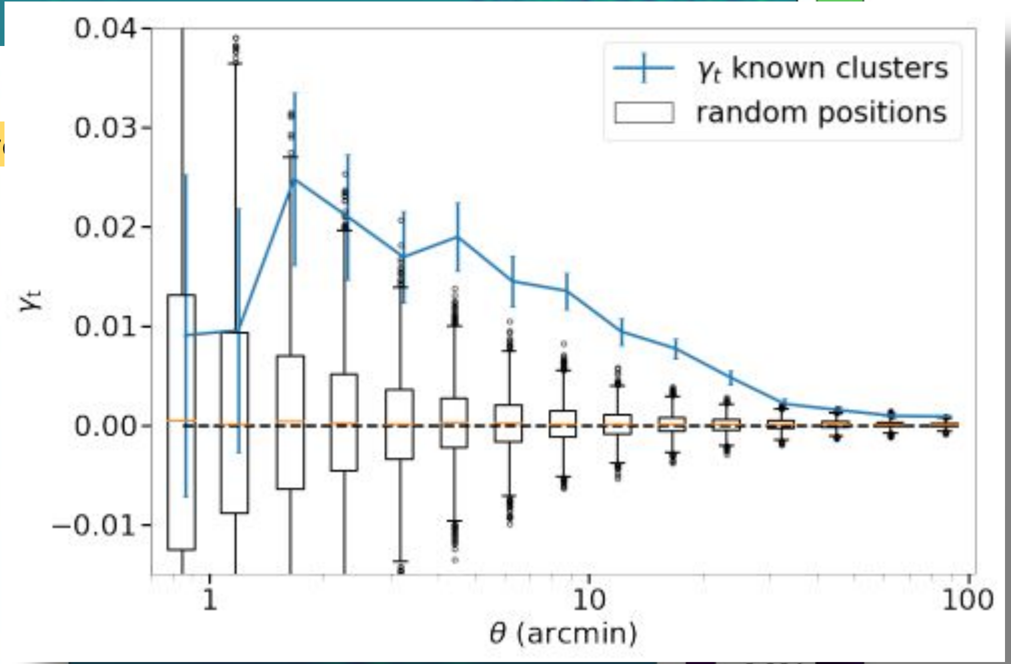

Guinot et al. (2022)

Peak counts

Study of systematic effects:

- Local shear calibration
- Baryonic effects
- Intrinsic alignments
- Redshift uncertainty

Number of peaks in WL overdensity (/ noise) map depends on cosmological parameters.

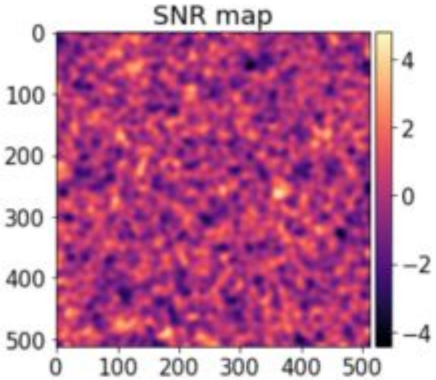

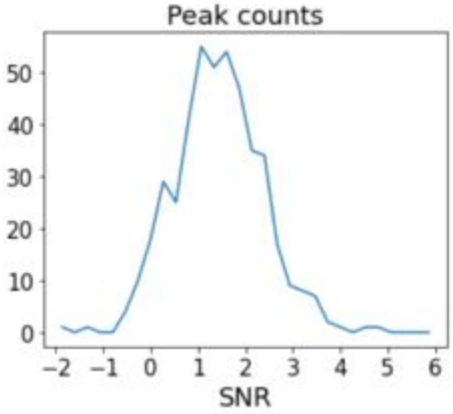

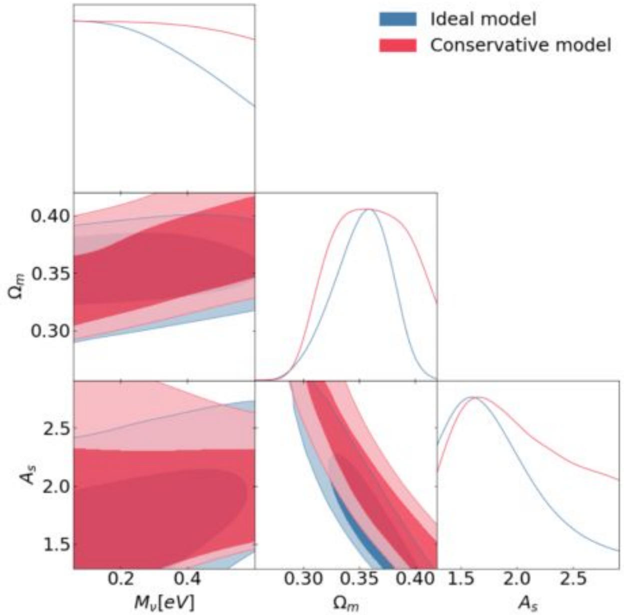

Ayçoberry et al, 2023

Follow-up work Tersenov, Beaumont et al.

Peak counts & local calibration

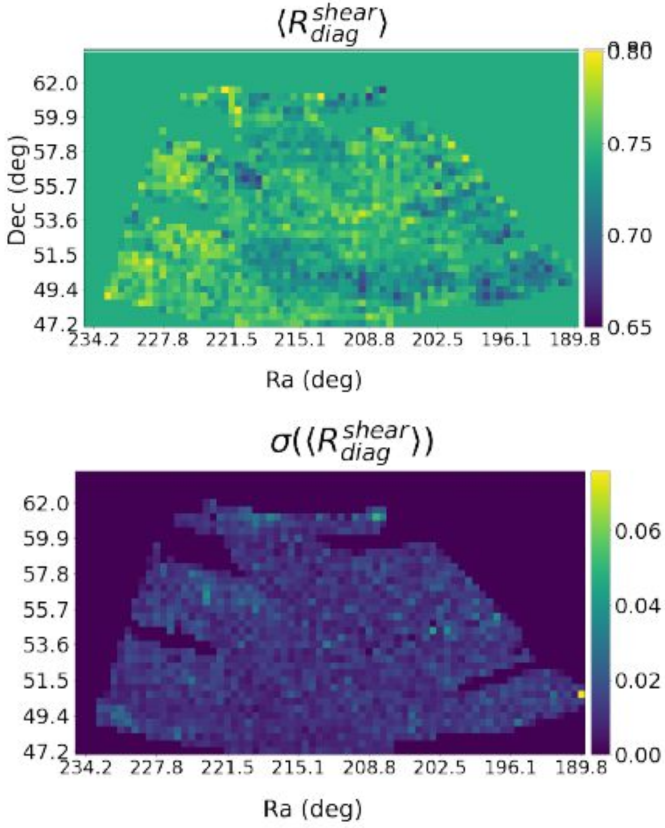

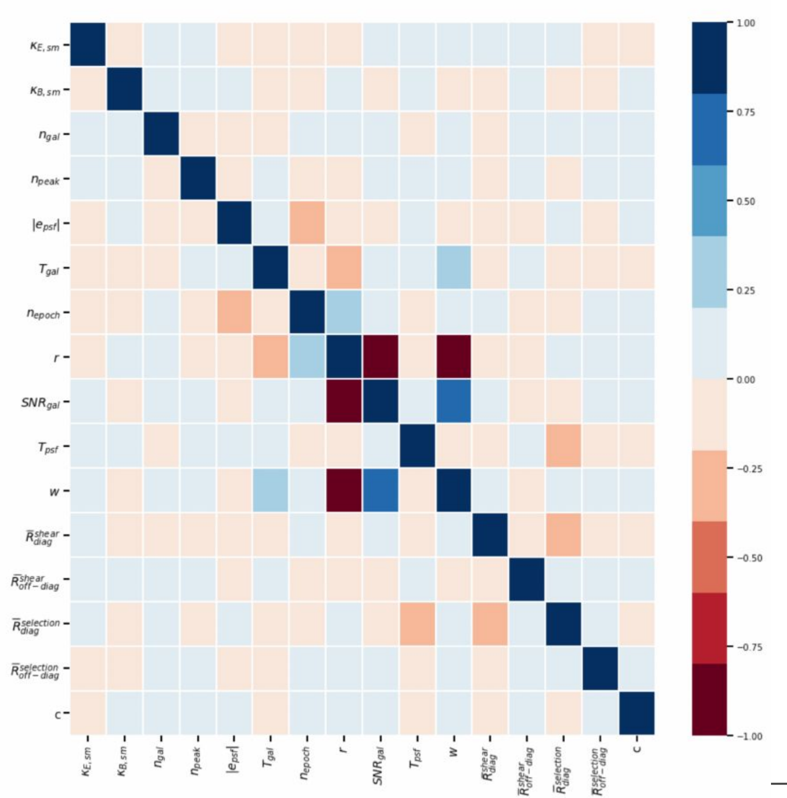

UNIONS & SDSS overlap

Combining spectroscopic and imaging information

From Fabian Hervas Peters

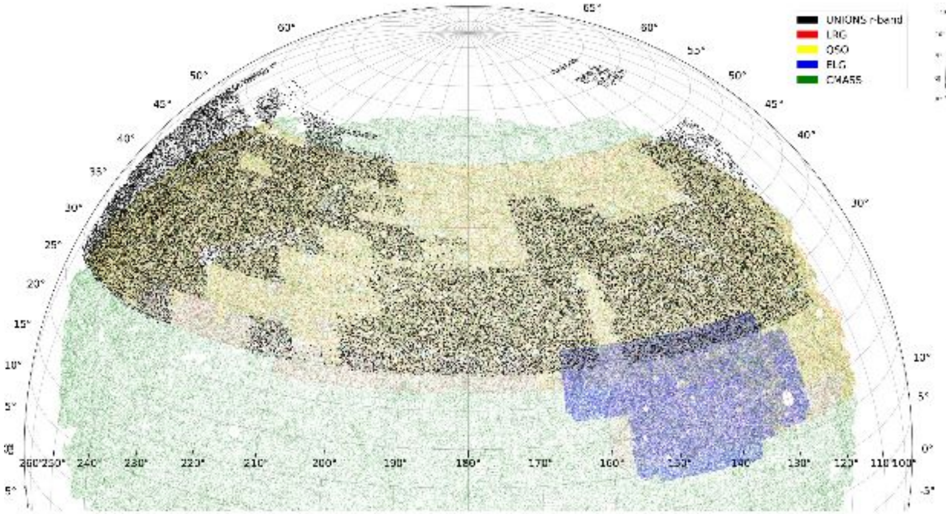

Northern Galactic Cap

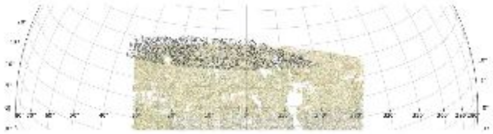

Southern Galactic Cap

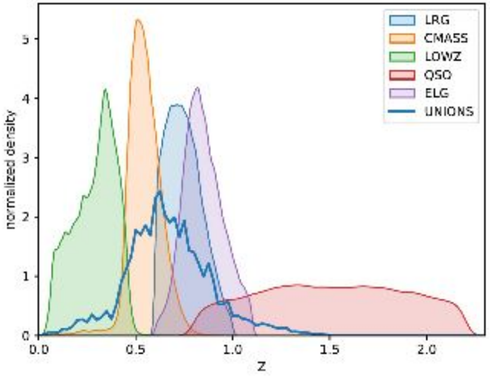

n(z) distribution

Intrinsic alignment

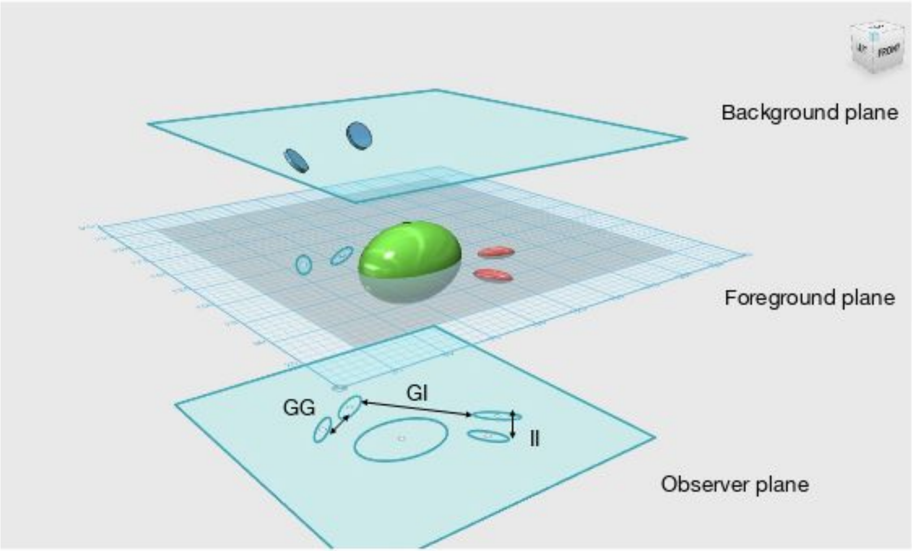

Intrinsic Alignment around a halo

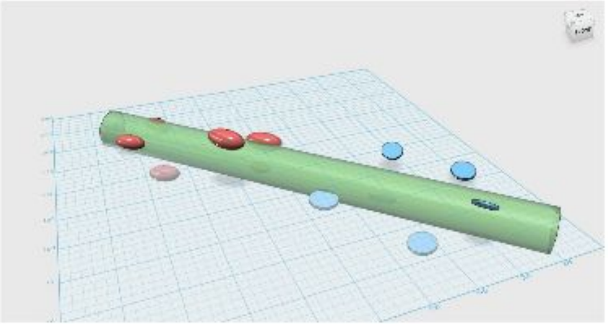

Intrinsic Alignment around a filament

$$\gamma = \gamma_I + \gamma_G$$

Intrinsic-Intrinsic

$$\langle \gamma\gamma \rangle = \underbrace{\gamma_G\gamma_G}_{\text{Cosmological}} + \overbrace{\gamma_I\gamma_I} + \underbrace{2\gamma_I\gamma_G}_{\text{Dominant intrinsic}}$$

Cosmological Dominant intrinsic

Source: Joachimi 2016, Galaxy alignments: An overview

Intrinsic galaxy alignment

UNIONS galaxies matched to SDSS galaxy pairs at same z.

CMASS

$\langle z \rangle$=0.55
shape sample=201 639
$\langle e \rangle$=0.216
$A_1 = 4.86 \pm 0.51$

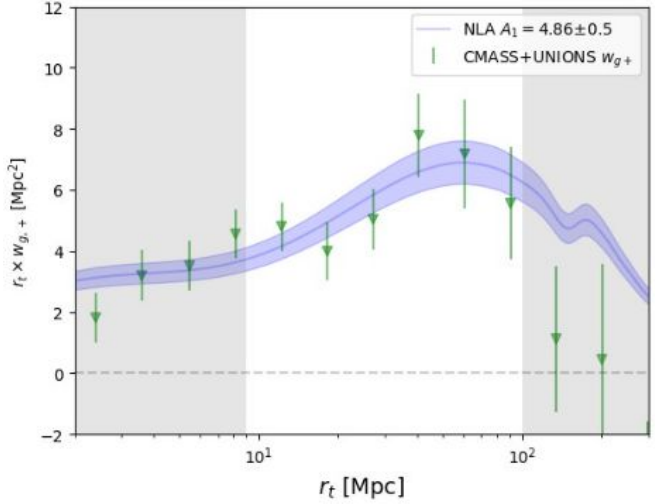

LRG

$\langle z \rangle$=0.74
shape sample=78 134
$\langle e \rangle$=0.265
$A_1 = 3.6 \pm 1.0$

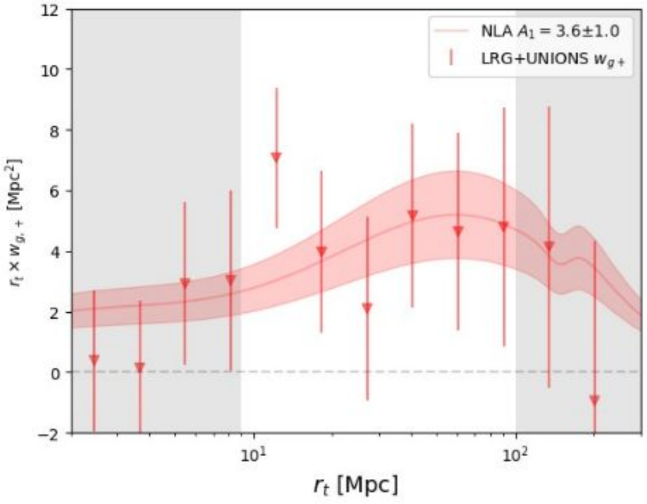

Hervas Peters, MK et al. (in prep)

Intrinsic alignment

Quasi-Stellar Objects (QSO)

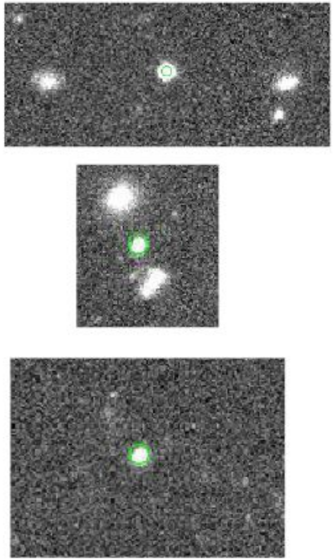

$\langle z \rangle$=1.5
shape sample=138 798
$\langle e \rangle$=0.33
$A_1 = 2.0 \pm 1.5$

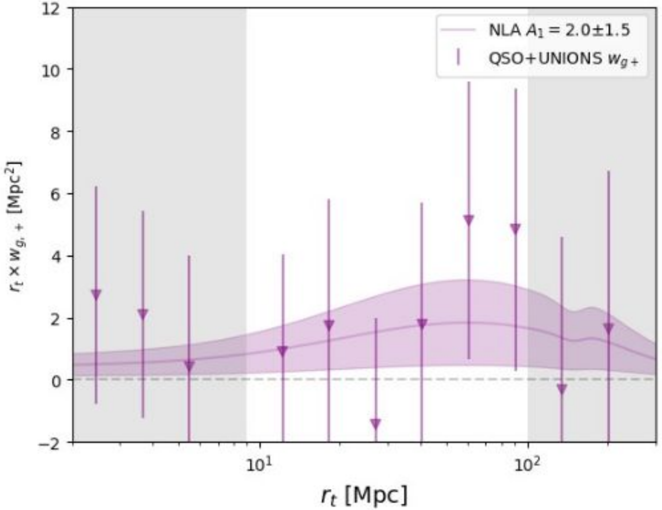

Hervas Peters, MK et al. (in prep)

Intrinsic alignment

Diagnosing Systematics

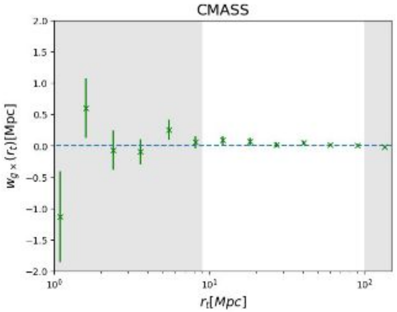

Deviation from 0:
χ^2: 3.5
1-p:0.83
Significance:0.2 σ

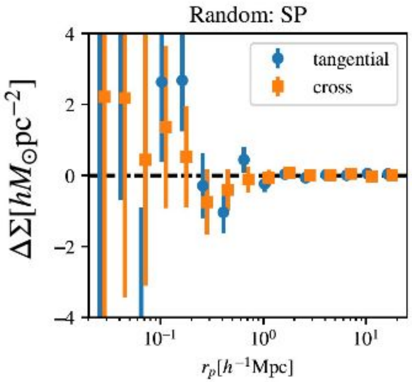

Excess surface mass density around random points
Source: Li et al. (in prep)

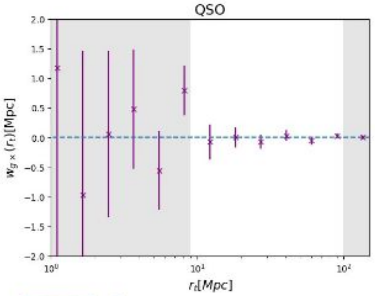

Deviation from 0:
χ^2: 2.24
1-p:0.944
Significance:0.06 σ

Deviation from 0:
χ^2: 6.9
1-p: 0.43
Significance: 0.78 σ

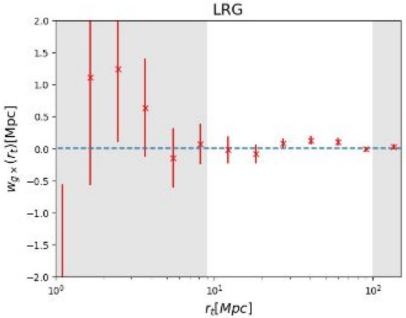

Weak-lensing by AGNs: BH - host halo mass relation

- Two AGN samples:
  - Liu et al (2019), SDSS DR7, 48,000 objects, 10,000 in UNIONS footprint.
  - Shen et al. (2011) and Wu & Shen (2022), SDSS DR16, includes DR7 catalogue, 206,000 objects, 55,000 in UNIONS footprint.
  - BH masses from broad-line regions.

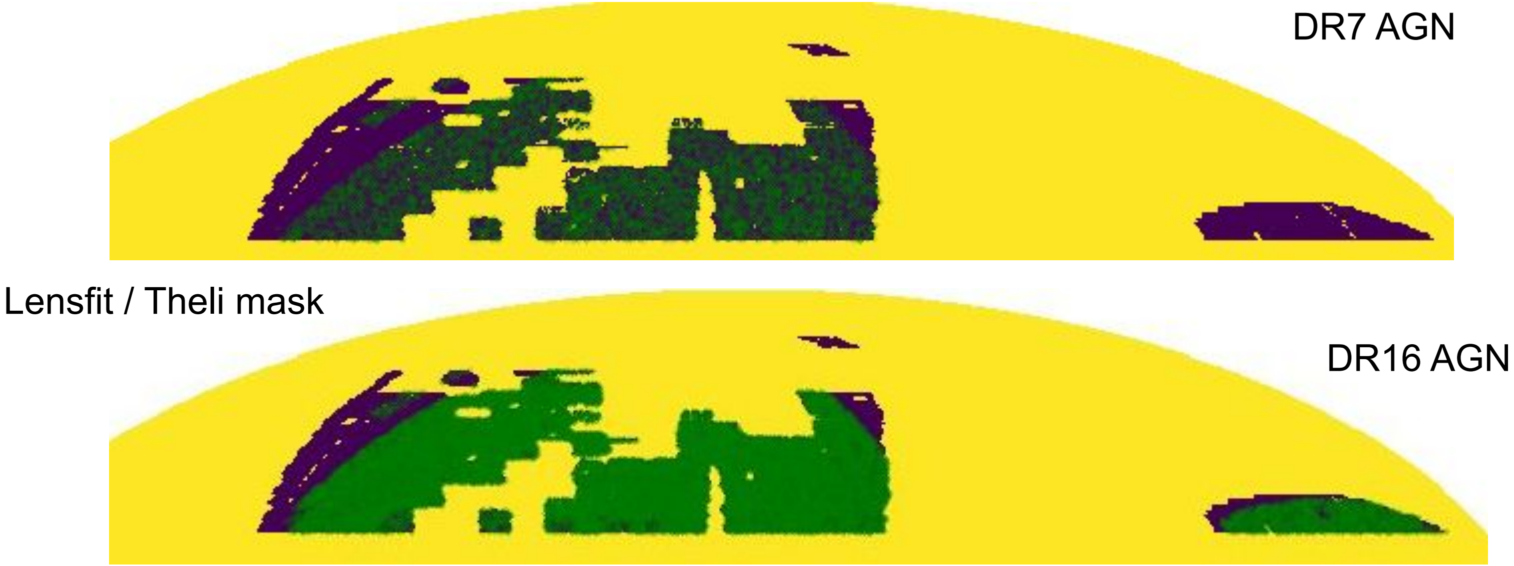

Weak-lensing by AGNs: BH - host halo mass relation

M - σ relation: linking black-hole mass to stellar velocity dispersion (proxy for halo mass).

Connection between black-hole growth and galaxy evolution.

Can we measure halo mass of black holes (AGNs) with weak-lensing?

Work with Li Qinxun, Luo Wentao, Zhang Ziwen, Fabian Hervas Peters, Elisa Russier and others.

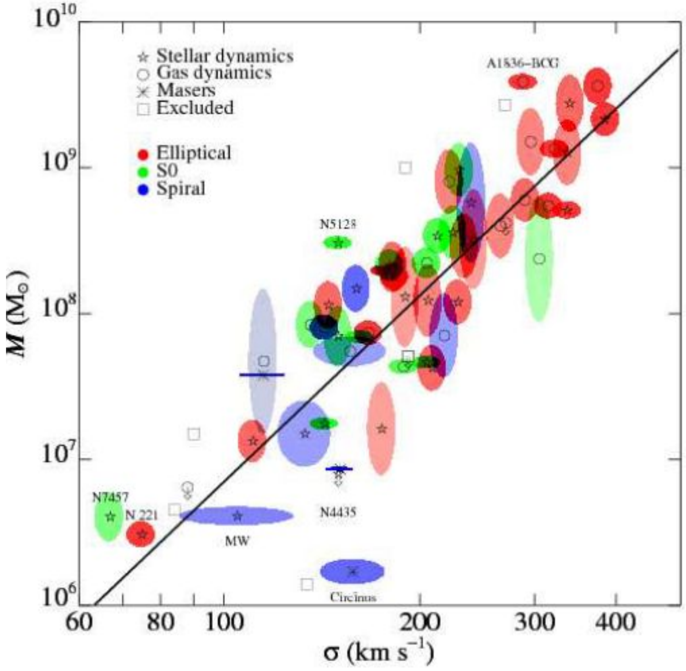

Weak-lensing by AGNs: BH - host halo mass relation

Fitting AGN halos with HOD (Halo Occupation Distribution) model.

Pyccl implementation:

$$\langle n_g(r)|M,a\rangle = \bar{N}_c(M,a)\left[f_c(a) + \bar{N}_s(M,a)u_{\rm sat}(r|M,a)\right]$$

$$\bar{N}_c(M,a) = \frac{1}{2}\left[1 + {\rm erf}\left(\frac{\log(M/M_{\rm min})}{\sigma_{\ln M}}\right)\right]$$

$$\bar{N}_s(M,a) = \Theta(M - M_0)\left(\frac{M - M_0}{M_1}\right)^\alpha$$

$$u_s(r|M,a) \propto \frac{\Theta(r_{\rm max} - r)}{(r/r_g)(1 + r/r_g)^2}$$

Weak-lensing by AGNs: BH - host halo mass relation

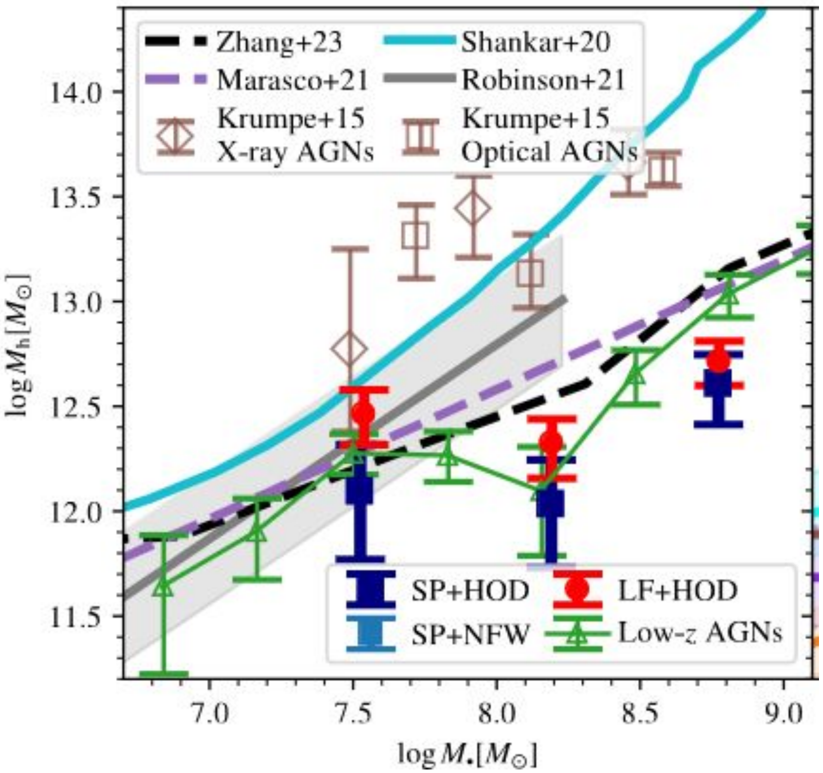

Li, MK et al. (in prep.)

Weak-lensing by AGNs: BH - host halo mass relation

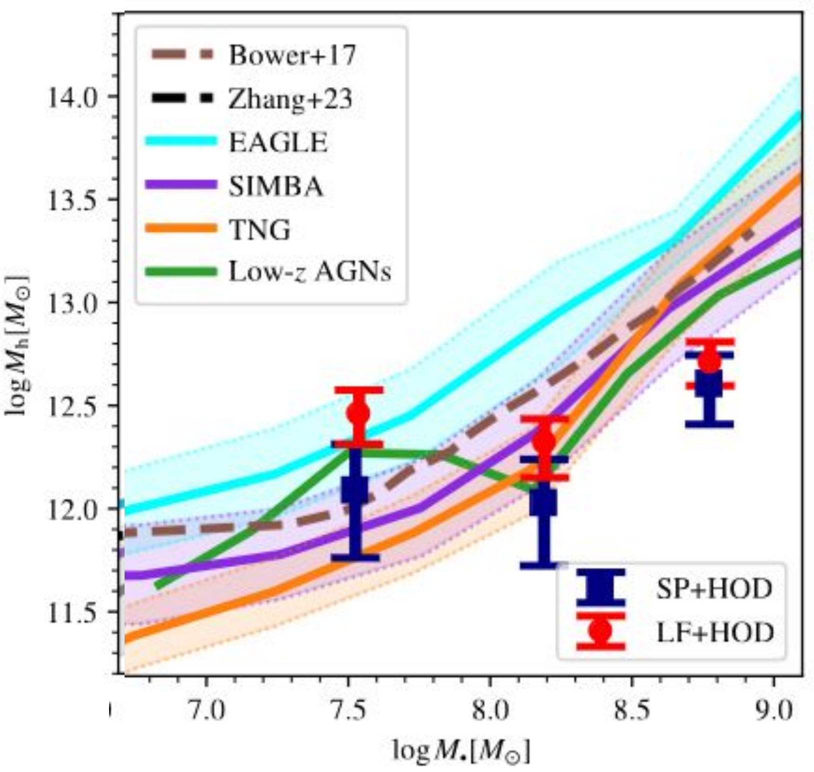

Li, MK et al. (in prep.)

UNIONS weak-lensing results (with ShapePipe)

A modular weak-lensing processing and analysis pipeline

Software paper	Farrens et al., 2022, A&A, 664, 141
Code & documentations	https://github.com/cosmostat/shapepipe
UNIONS first weak-lensing analysis	Guinot et al., 2022, A&A, 666, A162
Peak counts	Ayçoberry et al., 2023, A&A, 671, A17
Group & cluster masses	Spitzer et al., 2022, submitted to MNRAS
Dark-matter halo shapes	Robison et al., 2022, arXiv:2209.09088
Multi-CCD PSF model	Liaudat et al., 2021, A&A, 646, A27

In progress
Intrinsic galaxy alignment
Void lensing
Cosmic shear, constraints on Ω_m, σ_8, DE
Peak counts II
Lensing by AGNs, M_{BH} - M_{halo} relation
Analysis of CFHT P.I. data (rotating galaxy cluster, FRB field)

UNIONS weak-lensing: conclusions

https://unions.skysurvey.cc

- UNIONS: unique dataset for weak gravitational lensing:
    - Excellent image quality (median seeing < 0.7”)
    - Homogeneous survey depth thanks to adaptive observing strategy
    - Wide (4,800 deg^2), and deep (~ 10 galaxies $arcmin^{-2}$)
    - Large overlap with deep spectroscopic surveys (SDSS, eBOSS, DESI)

- Require dedicated image processing pipeline including calibration, systematic testing: ShapePipe; open source, tutorials, contribution & collaboration welcome

- Help understand relation between dark and luminous matter: group scaling relations, halo shapes, intrinsic alignments

Backup slides

with Goh, Hervas Peters, Guerrini, Baumont

Cosmological constraints

PSF systematics

- <= 10% of xi+, < statistical errors
- impact on cosmology TBC but probably small

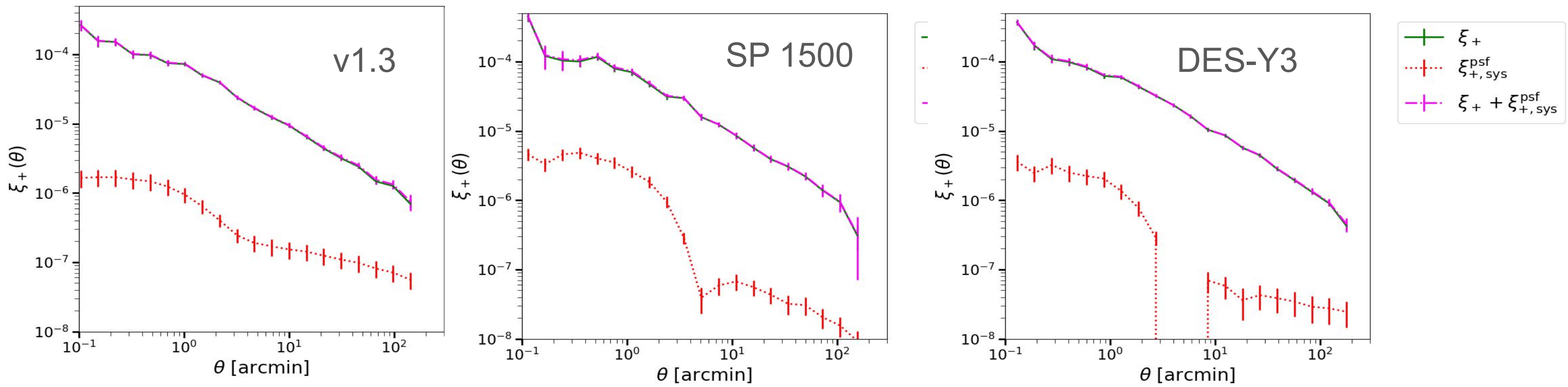

Cosmological const

C03 (purple): NL halofit

C04 (green): NL hmcode2020_feedback

C05 (blue): C04+ IA

C06 (pink): C05+delta_nz shifts

with Goh, Hervas Peters, Guerrini, Baumont

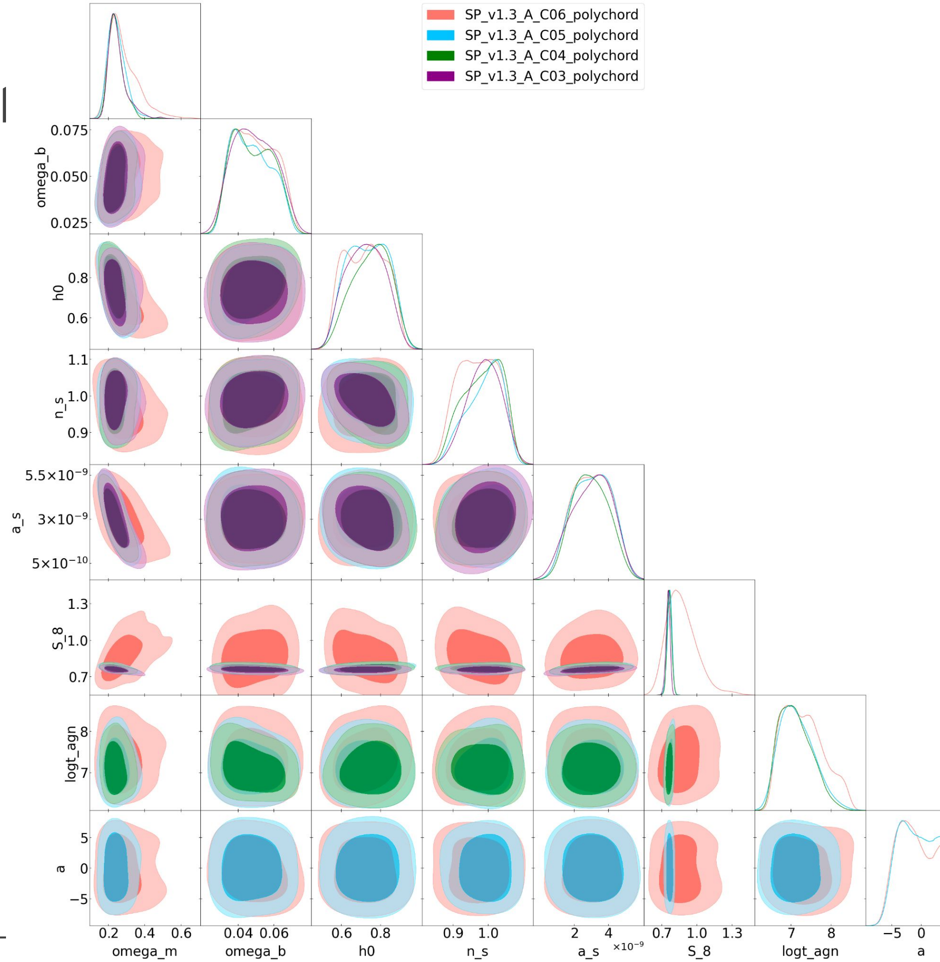

Cosmic shear?

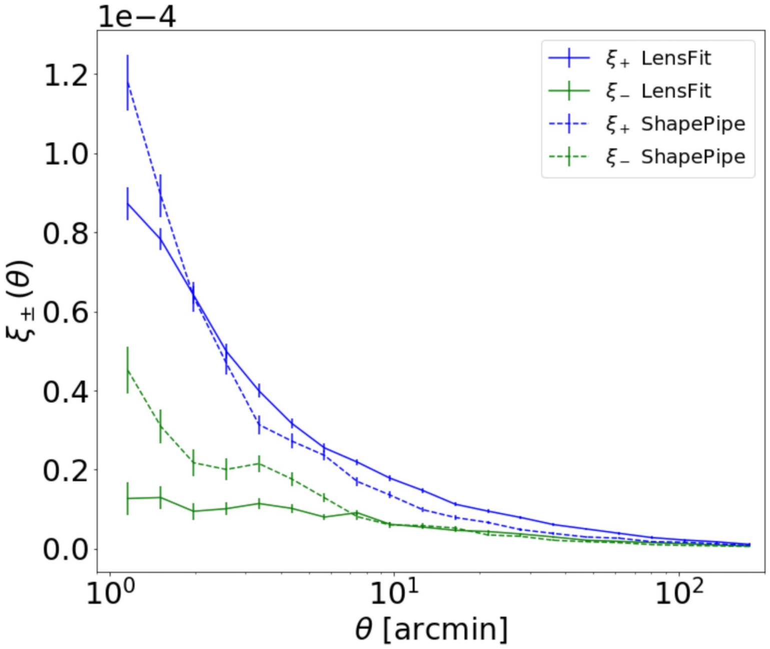

Void lensing

$$\frac{\rho_V(r)}{\overline{\rho}} - 1 = \delta_c \frac{1-(r/r_s)^\alpha}{1+(r/r_V)^\beta}$$

2 free parameters: δ_c and r_s

$$\Sigma_H(y) = 2\int_y^\infty \frac{(\rho_V(r)-\overline{\rho})r}{\sqrt{r^2-y^2}}dr$$

$$\Delta\Sigma = \overline{\Sigma(<r)} - \Sigma(r)$$

Citation: Hamaus N., Sutter P. M., Wandlet B. D., 2014, Phys. Rev. Lett., 112, 251302

Universal density profile

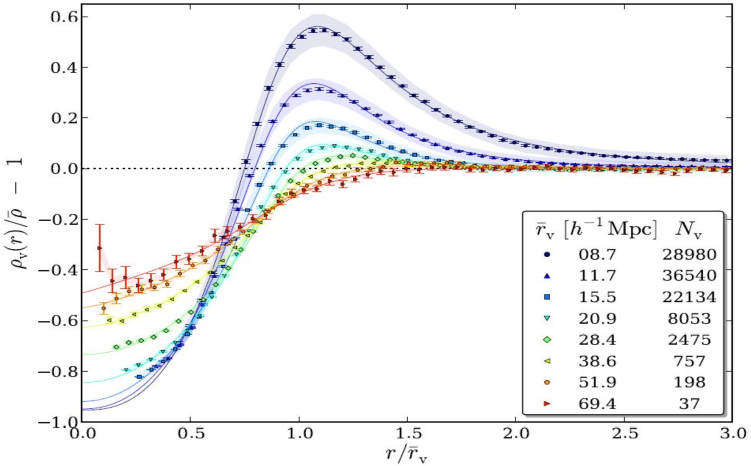

Fits of overdensity profiles of stacked simulated voids at redshift of 0. Source: (Hamaus et al. 2014)

Void lensing

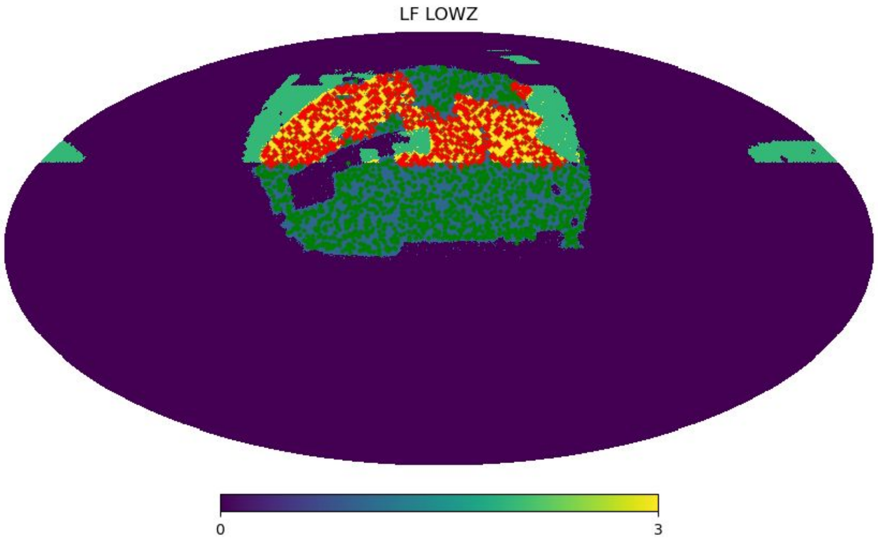

preliminary

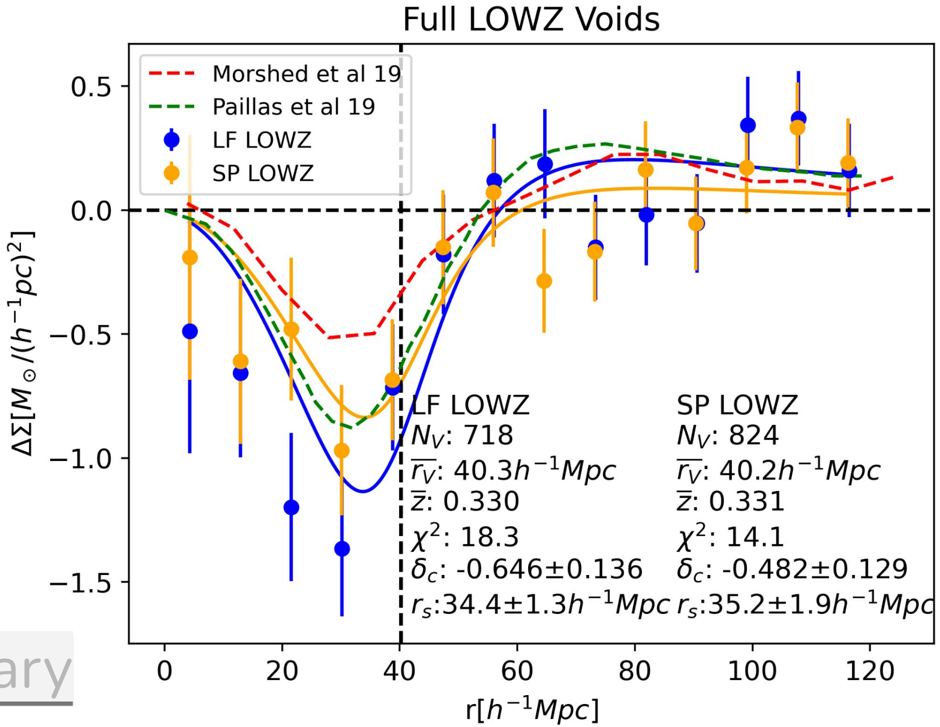

From Hunter Martin, Mike Hudson

Void lensing

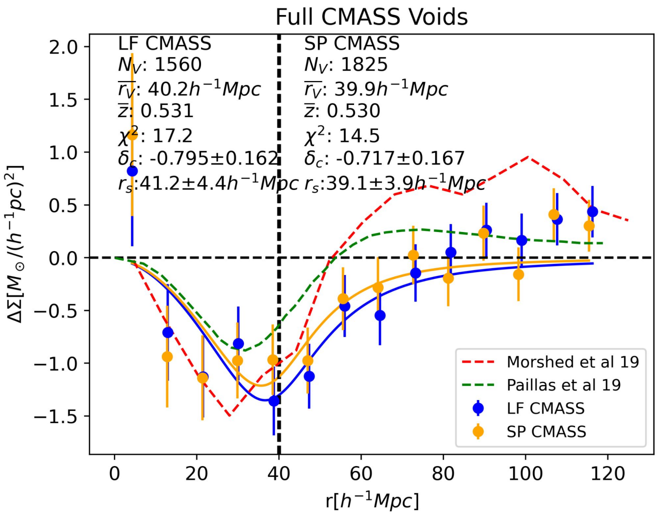

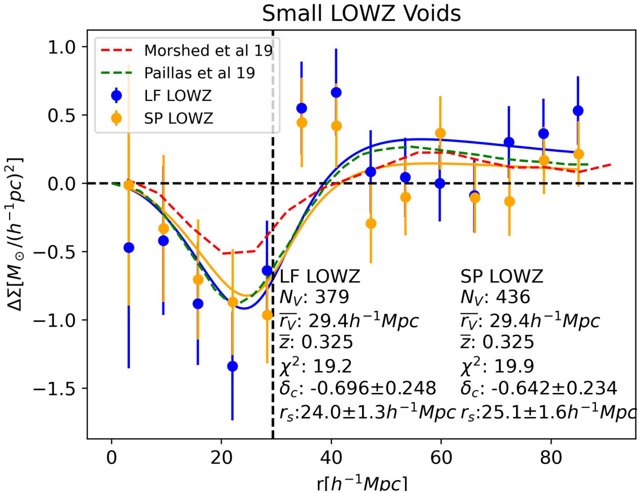

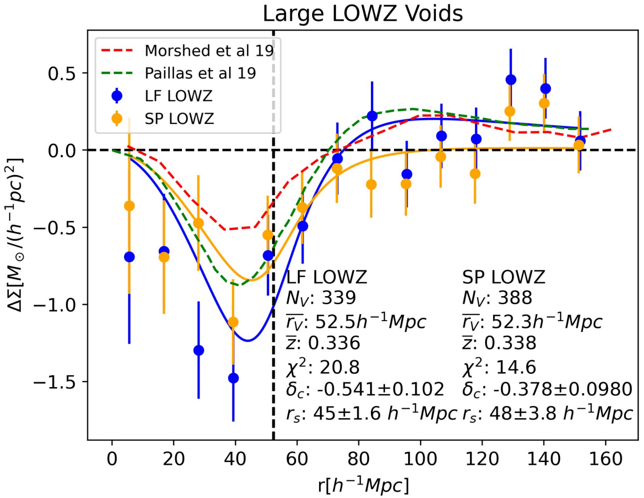

preliminary

From Hunter Martin, Mike Hudson

Group and cluster masses

Overdensity around SDSS redMaPPer groups.

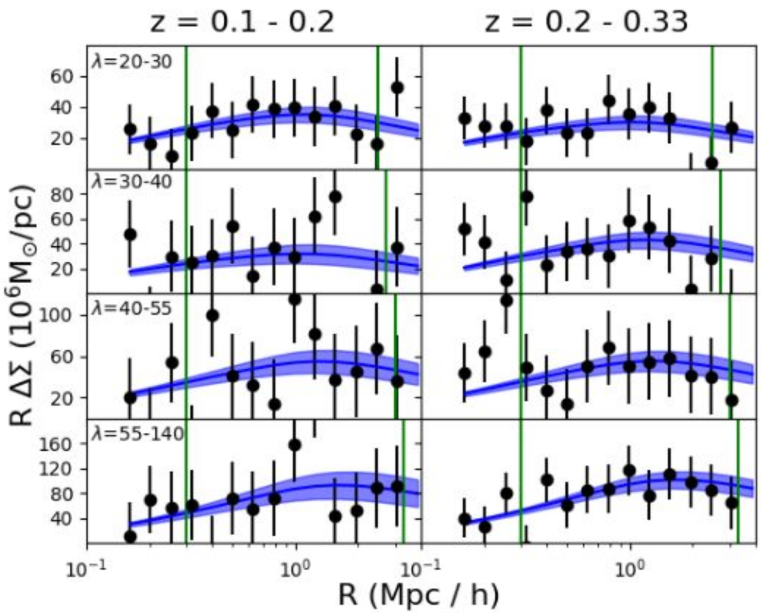

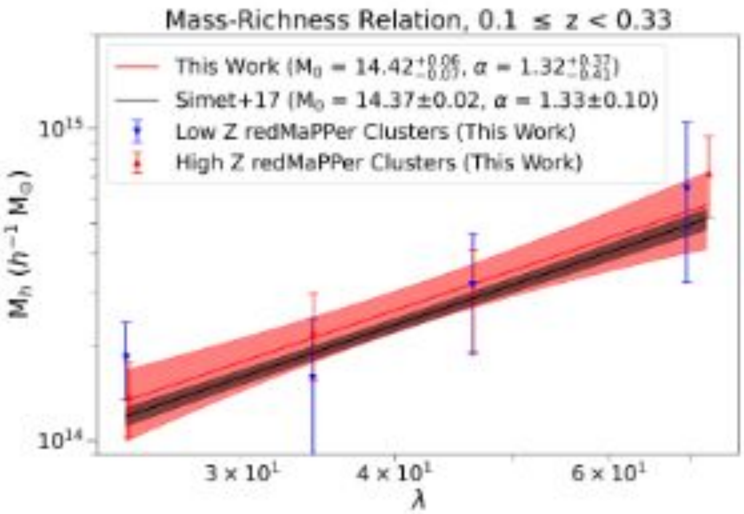

Spitzer et al. (2022)

Dark-matter halo shapes

WL halo profile of 146,000 SDSS DR7 Luminous Red Galaxies (LRGs).

Monopole.

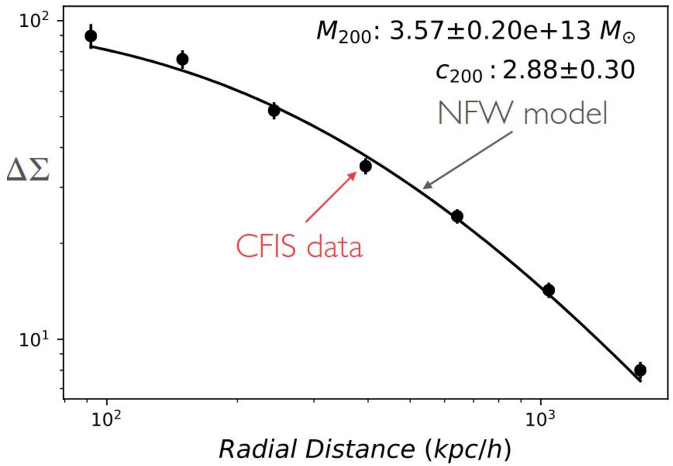

Can we measure the **quadrupole?**
→halo shape
Stack LRGs along galaxy orientation

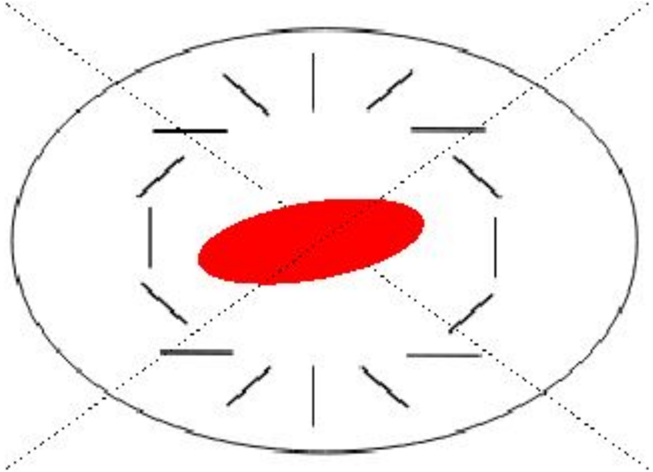

Robison et al, 2022

Dark-matter halo shapes

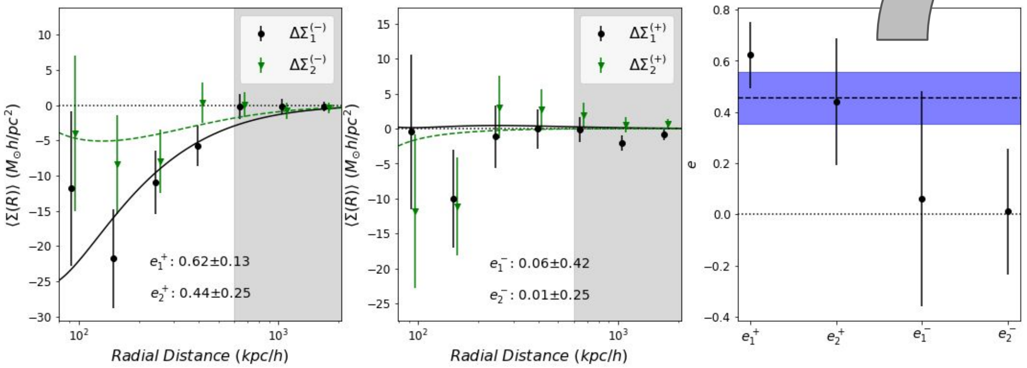

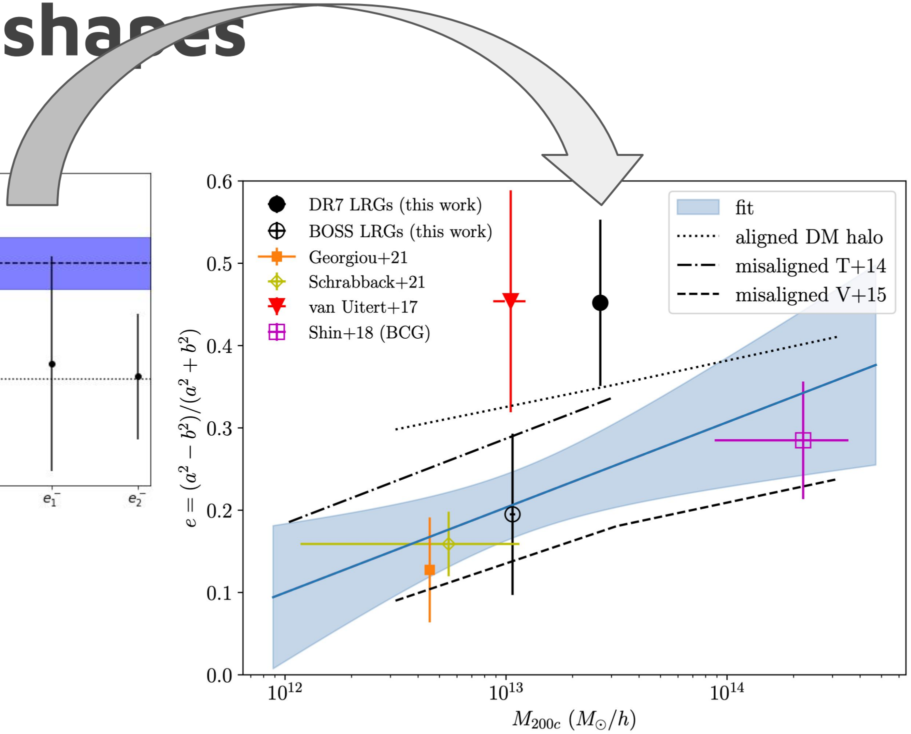

Robison et al, 2022

Time allocation

UNIONS = CFHT (u,r) + Pan-STARRS (i,z) + Subaru (g,z)

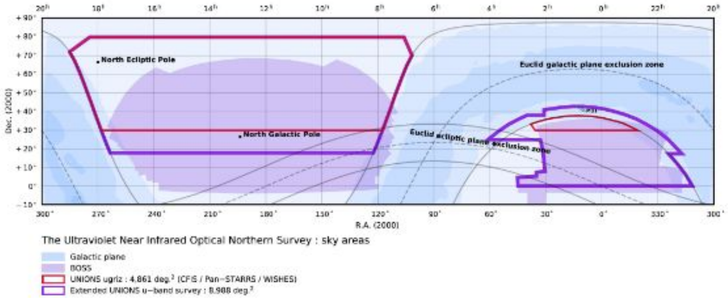

CFHT: 3 Large Programs (473 nights, 2015-2024)

- u : DEC>+0 on the SGC*, and DEC>+18 on the NGC*
- r : DEC>+30

**SGC = South Galactic Cap, NGC = North Galactic Cap*

Subaru: Waterloo-Hawaii-IfA G-band Survey

- g : DEC>+30 (20 nights, 2019-2024)

Pan-STARRS: (40% of PS1+PS2 since 2017)

- i : DEC>+30 (integration from NEOs search)
- z : +30<DEC<+42

Subaru: Wide Imaging with Subaru HSC of the Euclid Sky

- z : DEC>+42 (40 nights, 2020-2024)

UNIONS extension plan

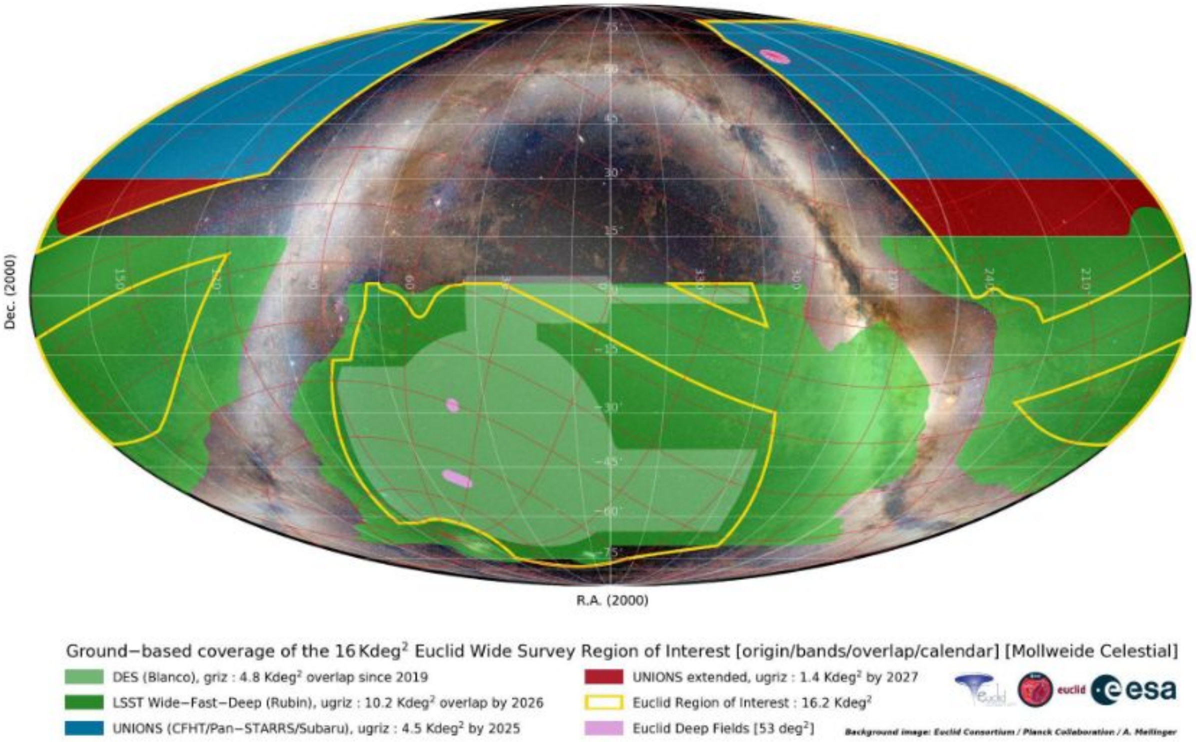

UNIONS publications

27 accepted peer reviewed publications so far: Resolved Stellar Populations Galaxy evolution Weak lensing

27. Robison, B., et al., 2023, in press, "The shape of dark matter haloes: results from weak lensing in the Ultraviolet-Near Infrared Optical Northern Survey (UNIONS)"
26. Lim, S., et al., 2023, MNRAS, in press, "Constraints on galaxy formation from the cosmic-infrared-background / optical-imaging cross-correlation using Herschel and UNIONS"
25. Smith, S., et al., 2023, ApJ, in press, "Discovery of a new Local Group galaxy candidate in UNIONS: Bo¨otes V"
24. Chu, A., et al., 2023, A&A, in press, A UNIONS view of the brightest central galaxies of candidate fossil groups
23. Bickley, R., et al., 2023, MNRAS, 519, 6149, "AGN in post mergers from the Ultraviolet Near Infrared Optical Northern Survey"
22. Ayc¸oberry, E., et al., 2023, A&A, 671, 17, "UNIONS : impact of systematic errors on weak-lensing peak counts"
21. Savary, E., et al . 2022, A&A, 666, 1 "A search for galaxy-scale strong gravitational lenses in UNIONS"
20. Chan, J. H. H., et al. 2022, A&A, 659, 140 "Discovery of Strongly Lensed Quasars in UNIONS"
19. Wilkinson, S., et al., 2022, MNRAS, 516, 4354, "The merger fraction of post-starburst galaxies in UNIONS"
18. Ellison, S., et al., MNRAS, 517, L92, "Galaxy mergers can rapidly shut down star formation"
17. Bickley, R., et al., 2022, MNRAS, 514, 3294, "Star formation characteristics of CNN-identified post-mergers in the Ultraviolet Near Infrared Optical Northern Survey (UNIONS)"
16. Farrens, S., et al., 2022, A&A, 664, A141, "A modular weak lensing processing and analysis pipeline"
15. Guinot, A., et al., 2022, A&A, 666, 162, "ShapePipe: a new shape measurement pipeline and weak-lensing application to UNIONS/CFIS data"
14. Sola, E., et al., 2022, A&A, 662, 124, "Characterization of LSB structures in annotated deep images"
13. Roberts, I., et al., 2022, MNRAS,509, 1342, "Ram Pressure Candidates in UNIONS"
12. Jensen, J., et al., 2021, MNRAS, 507, 1923, "Uncovering fossils of the distant Galaxy with UNIONS: NGC 5466 and its stellar stream"
11. Bickley, R., et al., 2021, MNRAS, 504, 372, "Convolutional neural network identification of galaxy post-mergers in UNIONS using IllustrisTNG"
10. Fantin, N., et al., 2021, ApJ, 913, 30, "The Mass and Age Distribution of Halo White Dwarf Candidates in the Canada-France Imaging Survey"
9. Liaudat, T., et al., 2021, A&A, A27, "Multi-CCD modelling of the point spread function"
8. Thomas, G., et al., 2020, ApJ, 902, 89, "The Hidden Past of M92: Detection and Characterization of a Newly Formed 17◦ Long Stellar Stream Using the Canada-France Imaging Survey "
7. Fantin N., et al., 2019, ApJ, 877, 148, "The Canada France Imaging Survey: Reconstructing the Milky Way from its white dwarf population"
6. Thomas, G., et al., 2019, ApJ, 866, 10, "Dwarfs or giants? Stellar metallicities and distances from ugrizG multi-band photometry"
5. Ellison, S., et al., 2019, MNRAS, 487, 2491, "A definitive merger-AGN connection at z~0 with CFIS: mergers have an excess of AGN and AGN hosts are more frequently disturbed"
4. Thomas, G., et al. 2019, MNRAS, 483, 3, "A-type stars in the Canada-France Imaging Survey - II. Tracing the height of the disc at large distances with Blue Stragglers"
3. Thomas, G., et al., 2018, MNRAS, 481, 4, "A-type stars in the Canada-France Imaging Survey I. The stellar halo of the Milky Way traced to large radius by blue horizontal branch stars"
2. Ibata, R., et al., 2017, ApJ, 848, 2, 129, "Chemical Mapping of the Milky Way with The Canada-France Imaging Survey: A Non-parametric Metallicity-Distance Decomposition of the Galaxy"
1. Ibata, R., et al., 2017, ApJ, 848, 2, 128, "The Canada-France Imaging Survey: First Results from the u-Band Component"